The case for persistent southwest-dipping Cretaceous convergence in the northeast Antilles: Geochemistry, melting models, and tectonic implications

Wayne T. Jolly[†]
Department of Earth Sciences, Brock University, St. Catharines, Ontario L2S 3A1, Canada

Edward G. Lidiak[§]
Department of Geology and Planetary Science, University of Pittsburgh, Pittsburgh, Pennsylvania 15260, USA

Alan P. Dickin[#]
Department of Geography and Geology, McMaster University, Hamilton, Ontario L8S 4M1, Canada

ABSTRACT

Constraints on the polarity of Cretaceous subduction in the Greater Antilles are provided through geochemical comparison between the erupted island arc lavas in central Puerto Rico and potential pelagic sediment reservoirs in the flanking ocean basins. Early Jurassic to mid-Cretaceous (185- to 65-Ma) sediment from the open Pacific on the southwest is dominated by pelagic chert, which is highly refractory and depleted with respect to incompatible elements. In comparison, mid- to Late Cretaceous (ca. 112- to 65-Ma) sediment from the younger Atlantic basin on the northeast was dominated by mixtures of two end members. These include (1) biogenic clay and carbonates with elevated light rare-earth element (LREE) abundances, negative MORB-normalized, high field-strength element (HFSE) anomalies, and low Zr/Sm; and (2) turbiditic detritus of upper continental crust composition with high LREE, comparatively shallow HFSE anomalies, and high Zr/Sm. Compositions of Puerto Rican arc basalts are inconsistent with incorporation of Pacific pelagic chert. Instead, patterns characteristic of high-Fe island arc tholeiites are reproduced by incorporation of up to 4% of a low-Zr/Sm biogenic sediment component of Atlantic origin, whereas patterns of low-Fe lavas require, in addition to biogenic sediment, introduction of up to 2% of a high-Zr/Sm crustal turbidite component. The Atlantic origin of all the subducted sediments indicates the polarity of subduction throughout the Cretaceous in the northeast Antilles was persistently southwest dipping. This conclusion is supported by the presence of a low-Zr/Sm suprasubduction zone component of Atlantic origin in Caribbean plateau basalts (91–88 Ma) from southwest Puerto Rico, which were erupted within the broad back-arc region of the Greater Antilles during intermediate stages of arc development.

Keywords: Caribbean, island arc, trace elements, pelagic sediments, upper continental crust.

INTRODUCTION

The Antilles Island Arc is subdivided naturally into two segments: (1) the extinct Cretaceous to Paleogene Greater Antilles in the north, including Cuba, Jamaica, Hispaniola, Puerto Rico, and the Virgin Islands, and (2) the volcanically active Lesser Antilles in the southeast, which rest on buried remnants of the older Mesozoic arc platform (Fig. 1A). The deeply dissected Greater Antilles segment of the arc preserves a continuous stratigraphic record of subduction along the plate boundary between North American and the Caribbean plates from Albian to mid-Eocene time (ca. 112–45 Ma; see, for example, Pindell et al., 2006), a total of over 70 my. Since oldest arc strata date uniformly from the early Cretaceous, and because geochemical and lithological sequences are similar in all the islands, the Antilles platform is considered to represent remnants of a once continuous volcanic arc chain that formed in the eastern Pacific or western Caribbean and subsequently drifted eastward, overriding the southwestern extension of the North Atlantic basin between the Americas, to its present position in the Caribbean basin (Donnelly, 1989; Pindell and Barrett, 1990). Within this framework, at least two contrasting tectonic models of Antilles evolution have developed. The models both involve a shift in the polarity of subduction from northeast to southwest dipping, but they differ fundamentally in the timing of the polarity shift and the mechanisms controlling it.

Plume-Centered Model

In one of these models (Fig. 1B), the Antilles arc is considered an extension of the northeast-dipping, Cordilleran-type subduction zone that bounded the western margin of the Americas between Albian and Campanian time (112–75 Ma; Lapierre et al., 1999; Kerr et al., 1999, 2002, 2003; Thompson et al., 2004; Kerr and Tarney, 2005; variants include Mattson, 1979; Schellekens, 1998; Smith et al., 1998). During that period, the Caribbean basalt plateau was extruded (92–88 my; Hauff et al., 2000; Kerr et al., 2002) west of the arc in the eastern part of the Pacific basin as the host Farallon plate (Fig. 1B) drifted eastward over the Galapagos hot spot. Shortly thereafter, in Campanian time, the plateau is thought to have reached the vicinity of the Cordilleran trench, where the thick buoyant basalt sequence choked off northeast-dipping subduction. As a result, subduction polarity was reversed and a southwest-dipping, Antillian-type subduction zone developed on the opposite flank of the arc platform (Lapierre et al., 1999; Thompson et al., 2004; Kerr et al., 2003; Fig. 1B). This model is consistent both

[†]Deceased
[§]E-mail: egl+@pitt.edu
[#]E-mail: dickin@mcmaster.ca

GSA Bulletin; July/August 2008; v. 120; no. 7/8; p. 1036–1052; doi: 10.1130/B26207.1; 12 figures; Data Repository item 2008003.

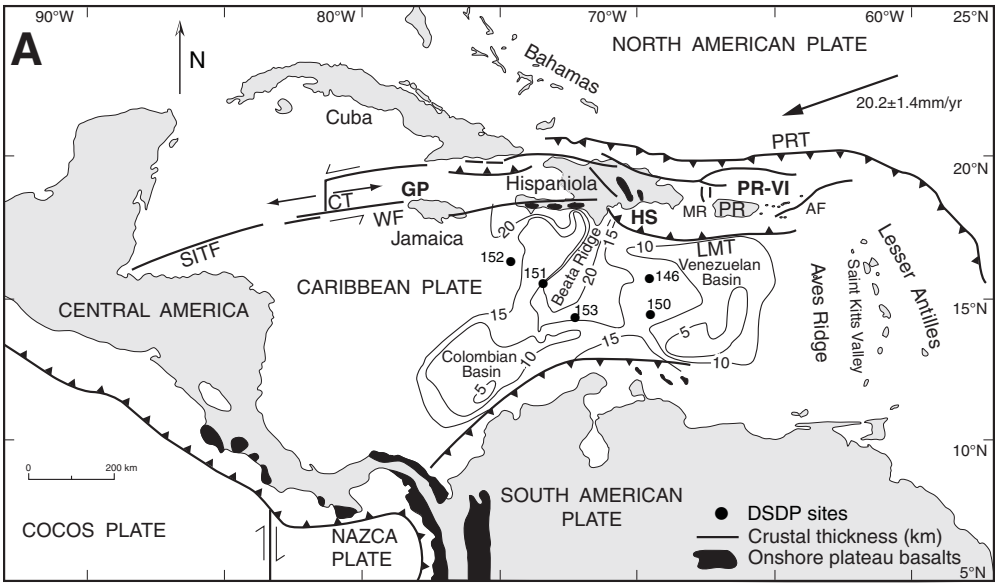

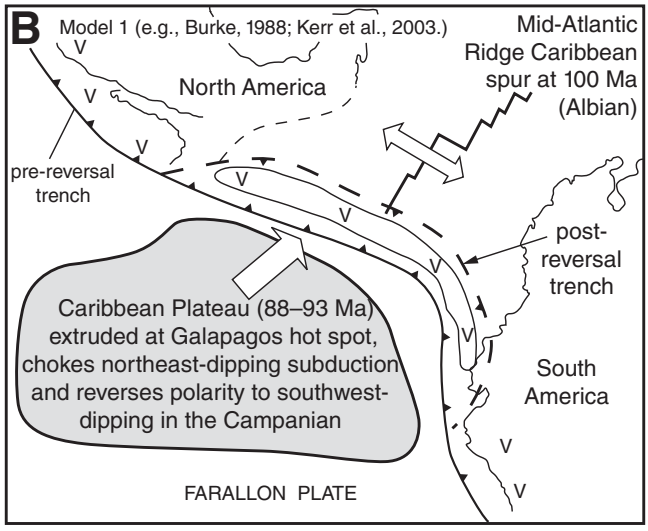

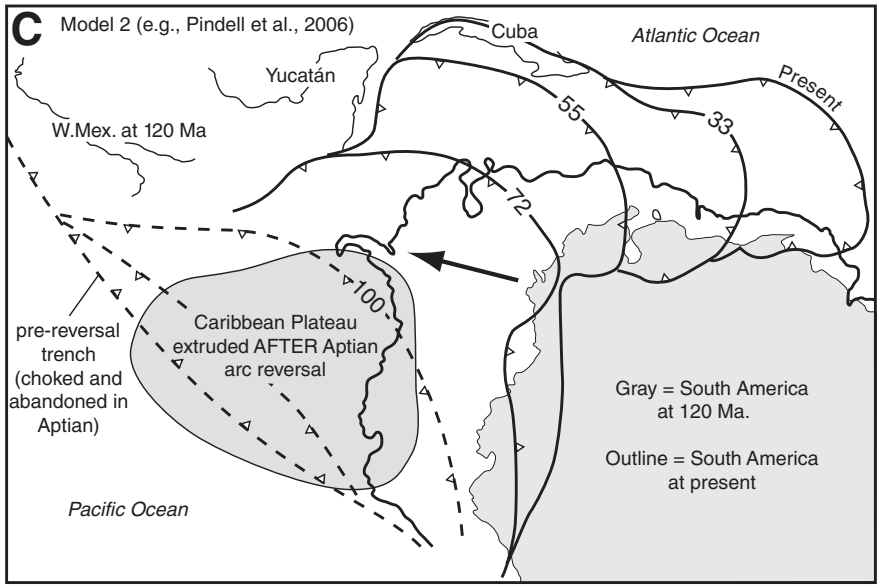

Figure 1. (A) Map of the Caribbean region showing principal structural elements of the tectonic boundary between the North American-Caribbean Plates (solid lines represent fault zones; teeth represent polarity of subduction zones). The vector, indicating motion of the Atlantic basin with respect to a stable Caribbean, is from Jansma et al. (2000). Contours in the Caribbean basin represent thickness (km) of oceanic crust (seismic velocity <5.0; Donnelly, 1989). Locations of deep sea drilling project (DSDP) drill sites within the Caribbean basalt plateau and onshore exposures of Caribbean plateau basalts are from Hauff et al. (2000) and Kerr et al. (2002). Additional features identified as follows: AF—Anegada Fault; CT—Cayman Trough spreading center; GP—Gonive microplate; HS—Hispaniola microplate; LMT—Los Muertos Trench; MR—Mona rift; PR—Puerto Rico; PRT—Puerto Rico Trench; PR-VI—Puerto Rico-Virgin Islands microplate; SITF—Swan Island Transform Fault; WF—Walton Fault. (B) Plume-centered model of tectonic development (Burke, 1988; Kerr et al., 2003; Kerr and Tarney, 2005) of the Cretaceous Antilles Island Arc, in which the Pacific (Farallon Plate) was subducted northeastward along a Cordilleran-type trench while at the same time (88–93 Ma; Kerr et al., 2002) the Caribbean basalt plateau was extruded farther west at the Galapagos hot spot. When the plateau reached the Cordilleran trench in the Campanian, its elevated buoyancy choked the trench and reversed the polarity of subduction to southwest dipping (see Pindell et al., 2006). (C) Mobile platform-centered Antilles model, in which the Caribbean basalt plateau was extruded in the Pacific following an Albian reversal of polarity from northeast to southwest dipping. The hypothetical position of the Antilles arc is shown for ca. 120, 100, 72, 55, and 33 Ma; the position of South America at 120 Ma is represented by the shaded outline, the modern position by the heavy bold line (modified from Pindell et al., 2006).

with (1) a Campanian age for Duarte overthrusting in southern Hispaniola, as suggested by Lapierre et al. (1999), and (2) the absence of a recognized suprasubduction zone trace-element signature in the basalt plateau outside of Puerto Rico (Kerr and Tarney, 2005).

Mobile Platform-Centered Model 2

In the other Antilles tectonic model (Fig. 1C), early stages of arc development also involved a brief initial period of Cordilleran-type, northeast-dipping subduction along the southwest flank of the arc platform (Pindell and Barrett, 1990). However, this phase is thought to have terminated relatively early, in the Albian, when the subduction zone was choked off by approach of a pre-Albian basalt plateau, the Duarte basement complex in southern Hispaniola (Draper et al., 1996; Lewis et al., 1999). Consequently, to compensate for continued convergence between the two adjacent plates, a new southwest-dipping subduction zone developed along the leading northeastern edge of the Farallon plate as it drifted northeastward into the slot between North and South America (Donnelly, 1989; Pindell and Barrett, 1990; Jolly et al., 1998, 2001; Kesler et al., 1991, 2005; Lewis et al., 1999; MacPhee et al., 2003; Iturralde-Vinent et al., 2006; Pindell et al., 2006; Marchesi et al., 2007). Seafloor magnetic anomalies (Pindell et al., 2006) indicate spreading between the Americas continued along a southwest spur of the mid-Atlantic Ridge until Campanian time (85–75 Ma). Consequently, Pindell (2004) suggested that Antilles tectonism involved long-term subduction of the active southwest spur of the Atlantic oceanic ridge system. Moreover, Pindell et al. (2006) proposed that opening of a slab window at depth along the subducted ridge culminated between 91 and 88 Ma with emplacement of the Caribbean Cretaceous mantle plume into the broad suprasubduction zone region behind the volcanic arc.

In the absence of unambiguous geographic or other physical evidence, an indirect approach is required to resolve the question of subduction polarity in the Antilles. One attractive avenue involves geochemical identification of the subducted sediment component and comparison with available sediment reservoirs (Jolly et al., 2006). Because Mesozoic sediments in the adjacent Pacific and Atlantic basins accumulated within distinctive and highly contrasting depositional environments, this approach has considerable potential in the Antilles. Jurassic to mid-Cretaceous sedimentation in the open Pacific on the southwest, for example, was dominated by accumulation of radiolarian chert (Montgomery et al., 1994) with high SiO_2 (95%–99%) and with low incompatible element concentrations compared with modern pelagic sediments. In contrast, the restricted and actively spreading Atlantic basin was dominated by shallow carbonate platform deposits mixed with variable proportions of detrital continental turbidites (Jolly et al., 2006; Marchesi et al., 2007). The primary objective of this investigation, therefore, is to determine from geochemical evidence which of the sediment reservoirs provided the sediment component incorporated by Antilles volcanic rocks. Although brief comparisons are made with adjacent areas, the primary focus is Cretaceous strata from central Puerto Rico (Fig. 2A), where a complete stratigraphic sequence (Fig. 2B) is exposed and mapped in detail (Bawiec, 2001).

GEOLOGICAL SETTING

The Puerto Rico–Virgin Islands microplate (PRVI) of Jansma et al. (2000) is located at the northeastern end of the ancient Greater Antilles island arc platform (Fig. 1A). It occupies the broad zone between the diffuse Puerto Rico Trench on the north and Los Muertos Trench on the south, and extends almost 450 km eastward from Mona Passage to the Anegada Fault Zone (Fig. 1A). Puerto Rico is dominated by an arched and deeply eroded volcanic core that consists of three tectonic terranes. Two of these, dating from Albian to mid-Eocene times, are genetically related and occupy the eastern two-thirds of the island, while a third, dating from the mid-Santonian to the mid-Eocene, comprises the southwestern third (Schellekens, 1991, 1998). The eastern terrains, to which this investigation is restricted, are separated from southwest Puerto Rico by the northwest-trending Greater Southern Puerto Rico Fracture Zone (GSPRFZ, Fig. 2A), which obscures stratigraphic relations. However, truncation of dominantly easterly arc trends in eastern Puerto Rico by northwest trends in the southwest indicates the terrains had separate tectonic histories (Dolan et al., 1991; Schellekens, 1998; Jolly et al., 2007).

The two tectonic terrains in eastern Puerto Rico, here called the northeast and central tectonic blocks, were juxtaposed during the mid-Santonian by at least 50 km of left-lateral, strike-slip displacement along the prominent Cerro Mula fault zone (Fig. 2A; Pease, 1968). Neither the basement or initial island arc strata are exposed in either block, but stratigraphic successions totaling up to 15 km thick are preserved in both (Jolly et al., 1998). In central Puerto Rico, there are five east-trending volcanic belts, corresponding with volcanic phases I through V (Fig. 2A–B), representing successive volcanic axes that gradually migrated northward by a total of almost 30 km from Albian to mid-Eocene times (ca. 112–45 Ma). Stratigraphic sequences of similar age and character are represented in adjacent northeast Puerto Rico and the Virgin Islands (Fig. 1A), except in those areas eruptive centers of all ages are concentrated within relatively narrow belts from 5 to 10 km in width.

Lower and Upper Albian volcanic belts in the central tectonic block (volcanic phases I and II; Fig. 2A–B) comprise two successive, 5-km–thick sequences dominated by low-K to medium-K, high-Fe island arc tholeiites, in the terminology of Gill (1981) and Arculus (2003). MgO and FeO* (total Fe calculated as FeO) content of the tholeiitic suite ranges from 4% to 8% and 8% to 14%, respectively. High-Fe strata are succeeded by an additional 5-km–thick Cenomanian to mid-Santonian volcanic belt (phase III) of medium-K to high-K, predominantly low-Fe basalts, with similar MgO but somewhat lower FeO* (from 6% to 12%). The volcanic succession in central Puerto Rico was interrupted by two disconformities that are sometimes correlated with an important Albian unconformity in Hispaniola (Lebron and Perfit, 1994; Draper et al., 1996; Lewis et al., 1999). However, the entire Albian to mid-Santonian arc sequence is conformable in the surrounding regions, including the western part of the central block (Mattson, 1968; Jolly et al., 1998; see Data Repository [Appendix Fig. 1][1]), northeastern Puerto Rico (Briggs, 1969; Briggs and Aguilar-Cortés, 1980; Fig. 2A), and in the Virgin Islands (Rankin, 2002; Fig. 1A). Hence, the disconformities in central Puerto Rico more likely reflect the presence of localized topographic highs of volcanic origin (Kaczor and Rogers, 1990).

Intermittent, predominantly subaerial volcanism continued to produce low-Fe–type volcanic strata during the Campanian (volcanic phase IV, ca. 85–75 Ma; Fig. 2B), but by Maastrichtian time, extrusive activity was replaced by granitoid plutonism (Donnelly, 1989; Schellekens, 1998; Lidiak and Jolly, 1996; Smith et al., 1998) accompanied by uplift and widespread erosion. Sporadic volcanism resumed during the Paleocene and continued until the mid-Eocene (volcanic phase V, ca. 45 Ma). As a result, the preserved volcanic sequence ends at an angular unconformity.

ANALYTICAL DATA BASE

Sample preparation was performed in mullite vessels to ensure minimal trace-element contamination. Complete major-element, inductively coupled plasma-emission spectrometer (ICP-ES) and trace-element, inductively coupled

[1]Data Repository item 2008003, Appendix Figures 1 and 2 and Appendix Tables 1–7, is available at http://www.geosociety.org/pubs/ft2008.htm or by request to editing@geosociety.org.

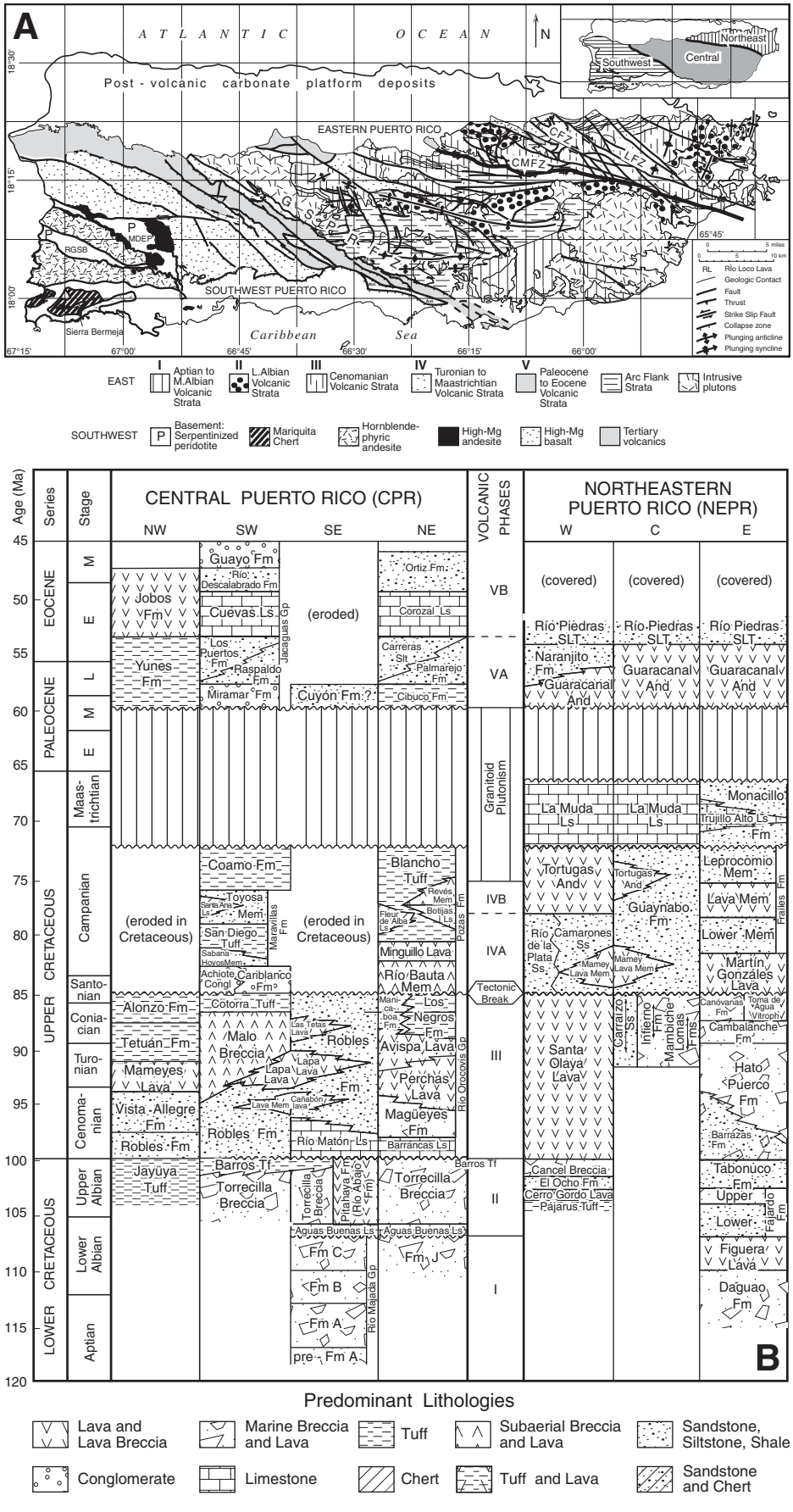

Figure 2. (A) Geologic map of Puerto Rico illustrating distribution of strata from volcanic phases I–V. CMFZ—Cerro Mula fault zone subdividing eastern Puerto Rico into central and northeast tectonic blocks, CFZ—Carraizo fault zone; LFZ—Leprocomio fault zone; GSPRFZ—Greater southern Puerto Rico fracture zone, subdividing western and eastern Puerto Rico (see inset). (B) Stratigraphic correlations in Puerto Rican arc-related strata (modified from Jolly et al., 1998, 2001; Schellekens, 1998). Unconformities and boundaries of volcanic phases I–V are from Jolly et al. (2006). The geologic time scale is from Gradstein et al. (2004).

plasma-mass spectrometer (ICP-MS) analyses of over 150 new samples from central Puerto Rican lavas, and seven samples of Mariquita Chert, representing Pacific Mesozoic pelagic sediment from southwest Puerto Rico (Fig. 2B), were analyzed commercially for this project, utilizing $LiBO_2$ fusion techniques. Analytical methods are summarized in Jolly et al. (2001, 2007). Duplicate analyses and deviations from standard curves indicate precision of analyses is within 1%–5% of the amount present or better for most trace elements. The new data extend the central Puerto Rico database to 234 complete analyses (Appendix Tables 1–7). Average unit compositions and Sr, Nd, and Pb isotope data are listed in Appendix Tables 1 and 2, respectively. Locations of central Puerto Rican units and their Mid-ocean Ridge Basalts (MORB)-normalized incompatible element patterns are shown in Appendix Figures 1 and 2, respectively.

The pervasive, low-temperature alteration characteristic of Antilles volcanic strata limits interpretation of measured geochemical signatures to some extent. For example, mobilization of water-soluble elements dispersed geochemical distribution patterns, masking slab-derived aqueous components contributed by metasomatizing fluids, and rendering problematic normative compositions and rock classifications based on K_2O (Peccerillo and Taylor, 1976; Le Maitre, 1981). Consequently, this study is restricted to major- and trace-element components that are stable in the presence of chloride brines, including HFSE, rare-earth elements (REE), and Th (Pearce and Parkinson, 1993). Large-ion lithophile elements (LILE; Rb, Cs, Ba, U, K, and Sr) are excluded except as general indicators of relative abundance (high, moderate, and low). Apart from the alkalis, major-element oxides form well-defined fields when plotted against more immobile components, such as Al_2O_3, indicating that measured abundances reflect original

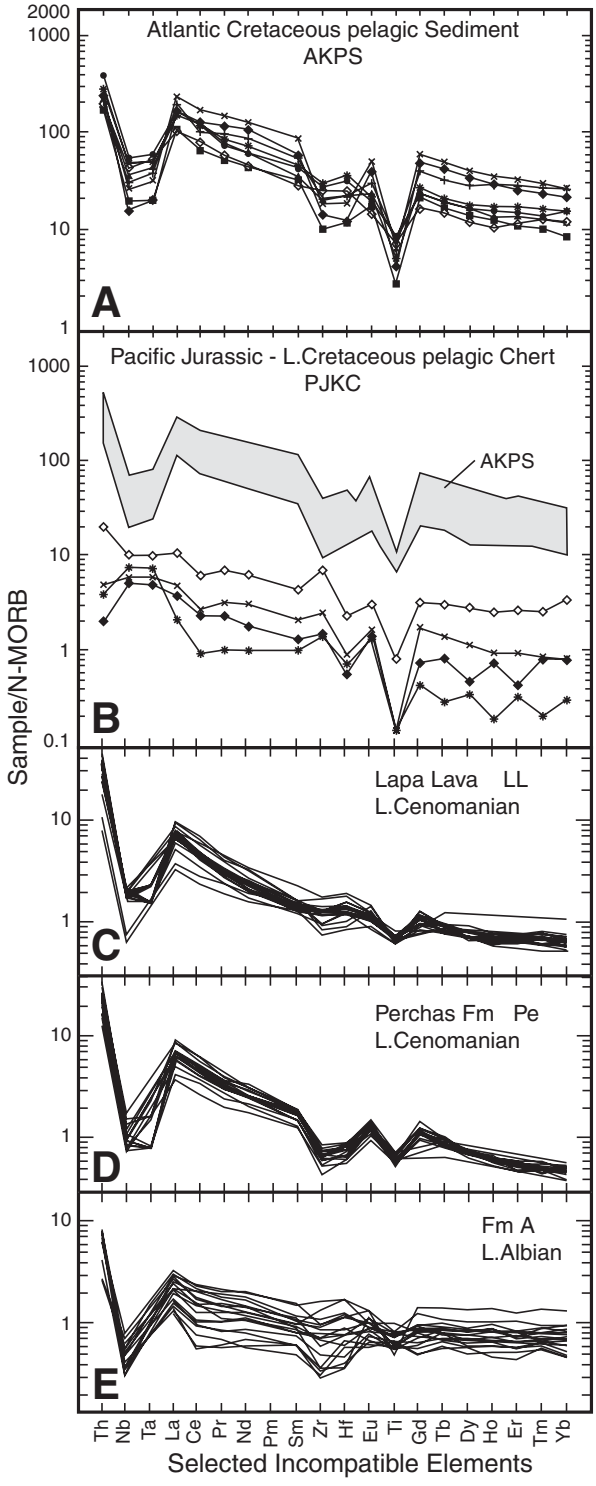

Figure 3. MORB-normalized (Sun and McDonough, 1989) incompatible element patterns of (A) Atlantic Cretaceous pelagic sediment (AKPS) from DSDP drill cores, (B) Pacific Jurassic to Lower Cretaceous pelagic chert (PJKC), represented by samples from the Mariquita Chert (95%–99% SiO_2) from southwest Puerto Rico. Also shown for comparison are patterns of samples from the (C) low-Fe Lapa Lava and (D) high-Fe (island arc tholeiitic) Perchas Formation, both from volcanic phase III, and (E) Formation A from volcanic phase I; patterns of other central Puerto Rican units are presented in Appendix Figure 2.

compositions. To minimize scatter introduced by hydration, data in diagrams are recalculated on an anhydrous basis to 100%. Volcanic classes are based on SiO_2 abundance (Peccerillo and Taylor, 1976) and include (mafic) basalt (SiO_2 = 45%–53%) and basaltic andesite (53%–57%), (intermediate) andesite (57%–63%), and (felsic) dacite (63%–70%) and rhyolite (>70%).

POTENTIAL PELAGIC SEDIMENT RESERVOIRS

Pacific Mesozoic pelagic sediment is represented (Appendix Table 7) in southwestern Puerto Rico by radiolarian chert (Mariquita Chert; Mattson, 1960; Fig. 2A) of Early Jurassic (Pleinsbachian) to Early Cretaceous age (185–65 Ma; Montgomery et al., 1994). Ranging in SiO_2 from 96% to 100%, the chert is highly refractory, with N-MORB–normalized incompatible element concentrations at least two orders of magnitude more depleted than Cretaceous sediment from the contemporary Atlantic basin (cf. Fig. 3A–B), rendering it ineffective as a mantle contaminant. Most samples have positive normalized Nb anomalies resembling ocean island basalt (OIB), indicating a source dominated by Pacific volcanic ash rather than continental turbidites as in the Atlantic.

Atlantic Cretaceous pelagic sediment (AKPS; Fig. 3A) is represented by ten samples from Deep Sea Drilling Project (DSDP) drill cores from sites 105 and 417D in the eastern North Atlantic (Donnelly, 1978; Donnelly et al., 1978; Jolly et al., 2006; Appendix Table 7). The oldest samples (Fig. 4A) are dominated by biogenic sediments, including limestone and calcareous claystone. Carbonate was gradually supplanted during the Late Cretaceous and Cenozoic, first by black and green biogenic clay and then by detrital zeolitic claystone. MORB-normalized patterns of Atlantic sediments are characterized by well-developed, negative Nb-Ta, Zr-Hf, and Ti anomalies closely resembling patterns of Antilles Island Arc lavas. On variation diagrams, the sediments form elongate fields (Fig. 4B–C) subparallel with the fields of global subducting sediments (Global Subducting Sediment Composition [GLOSS]; Plank and Langmuir, 1998). However, Atlantic sediments consistently have slightly elevated values for both Nb/Zr (~0.1) and La/Sm (between 4 and 6) compared with GLOSS. In earlier geochemical models (Jolly et al., 2001, 2006), sediment proportions in Antilles lavas were estimated from average bulk sediment compositions. However, both global and Atlantic pelagic sediments have wide ranges in La/Nb (from 1.5 to over 10) and Zr/Sm (5–40), indicating mixing between two distinctive end members. The low La/Nb-high Zr/Sm end member resembles the average upper

continental crust (UCC) of Taylor and McLennan (1985, as modified by Plank and Langmuir, 1998), whereas the high-La/Nb–low-Zr/Sm end member is dominated by HFSE-poor, biogenic clay and carbonate. Hence, to adequately characterize sediment mixing processes involved in south-dipping subduction of the Atlantic basin, three-component mixing models, involving the wedge source, biogenic sediment, and an upper continental crust component, are introduced in this investigation.

VOLCANIC GEOCHEMISTRY IN THE NORTHEAST ANTILLES

Petrography

Puerto Rican volcanic rocks are predominantly porphyritic, although the less siliceous samples from most units tend to be aphyric or relatively phenocryst poor and, therefore, more closely represent melt compositions. Many samples contain as much as 20% phenocrysts set in a matrix of feathery to spherulitic, devitrified glass together with small proportions of magnetite and apatite. Plagioclase and ferroaugite, up to 0.5 cm in length, are present in all units, but Cenomanian strata from volcanic phase IV contain, in addition, up to 5% by volume of brown hornblende. Samples from most intermediate and felsic units are normally clouded with abundant, commonly subtrachytic, plagioclase microlites measuring <0.5 mm in length. Large glomeroporphyritic augite clusters, up to 1 cm in diameter, are characteristic in Upper Albian basalts from volcanic phase II (Torrecilla and Pitahaya Formations, Fig. 2B) and in Cenomanian basalts from phase III (Perchas Formation, Fig. 2B). The abundance of plagioclase in all the rocks is consistent with low-pressure, subvolcanic, fractional crystallization of the original high-pressure island arc melts.

Major Elements

Basalts and Andesites

Fields of individual stratigraphic units in central Puerto Rico concentrate in SiO_2-FeO*/MgO plots (Fig. 5) along the tholeiite-calcalkaline boundary of Miyashiro (1974), with basalts predominantly in the tholeiitic and andesites in the calcalkaline field. Consequently, basalts tend to overlap the high-Fe and moderate-Fe suites of Arculus (2003), whereas andesites and more felsic lavas overlap the low-Fe and moderate-Fe suites. Although individual units from both suites normally have diagonal fields that slope upward to the right, consistent with fractional crystallization of clinopyroxene and olivine, low-Fe units are significantly offset toward

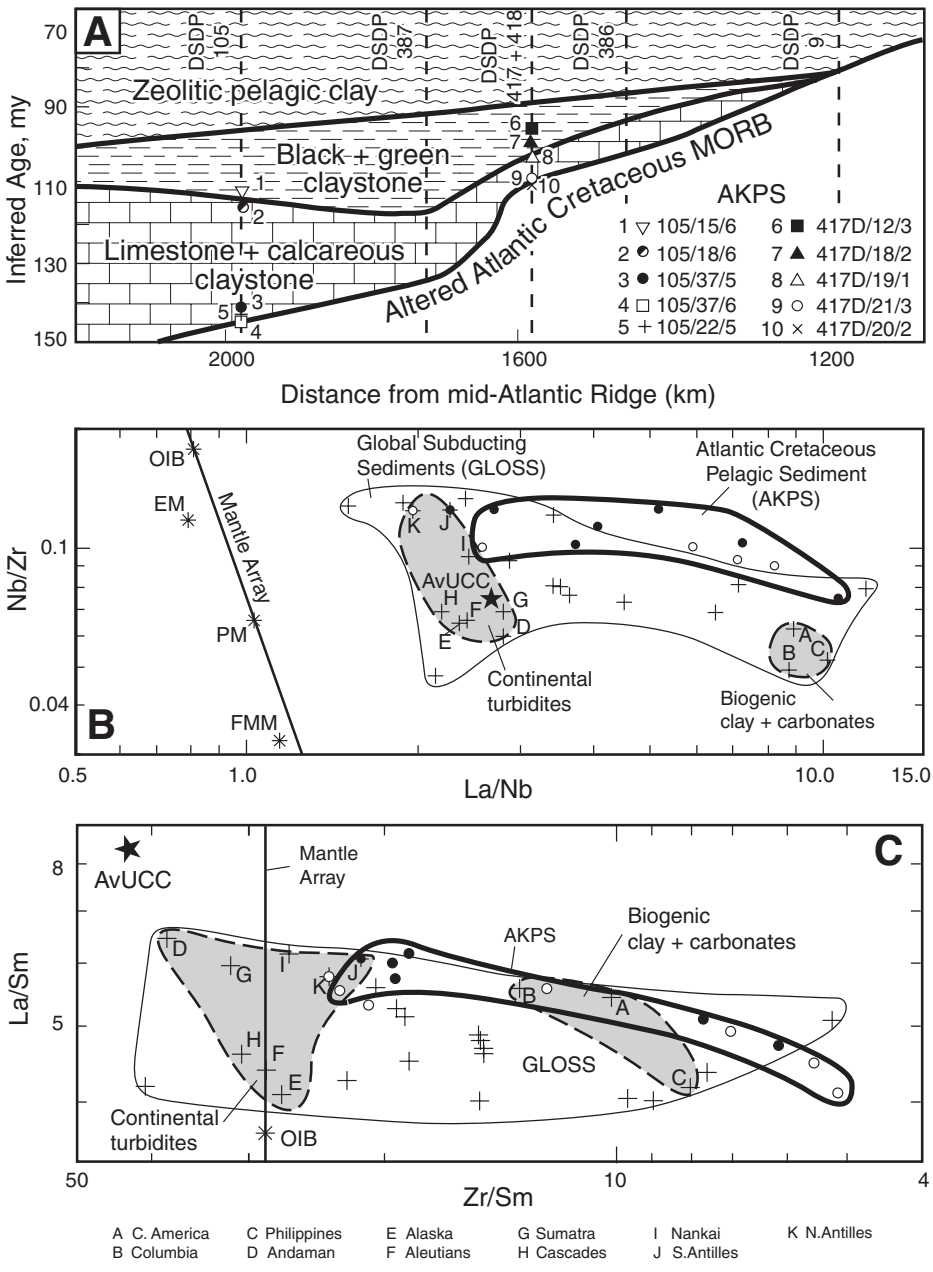

Figure 4. (A) Schematic profile of southwest Atlantic, indicating paleontologic ages of Cretaceous pelagic sediments relative to distance from the mid-Atlantic ridge, and the distribution of altered Atlantic Cretaceous MORB and pelagic sediment facies (compiled from data of Donnelly, 1978). (B)–(C) Geochemistry of Atlantic Cretaceous pelagic sediments (AKPS) compared with Cenozoic global subducting sediments (GLOSS; Plank and Langmuir, 1998). The shaded fields represent sediments dominated by turbidites of upper continental crust origin (left) and biogenic clay and carbonates (right). (B) La/Nb versus Nb/Zr. (C) La/Sm versus Zr/Sm. Upper continental crust (UCC) is from Plank and Langmuir (1998) and Taylor and McLennan (1985).

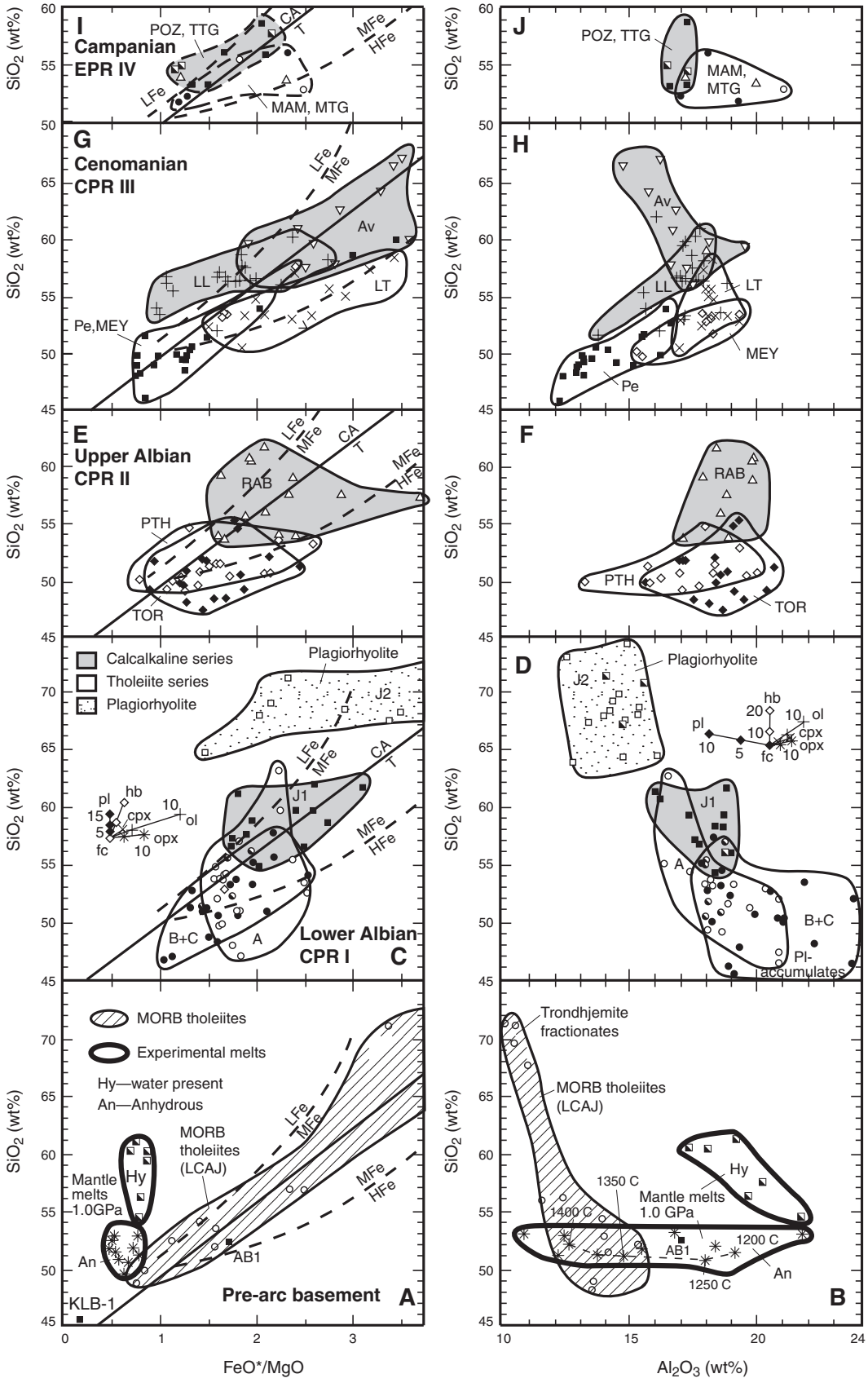

Figure 5. Covariation of SiO_2 with FeO*/MgO and Al_2O_3 in volcanic rocks from central Puerto Rico, compared with the pre-arc basement in southwest Puerto Rico. Unit codes as in Figure 7; symbols include LFe, MFe, and HFe—low-Fe, moderate-Fe, and high-Fe suites of Arculus (2003); CA and T—calcalkaline and tholeiite series of Miyashiro (1974); low-Fe units are shaded. Volcanic phases I to III in central Puerto Rico are denoted as CPR I, CPR II, and CPR III; phase IV, identified as EPR IV, includes strata from both central and northeast Puerto Rico. Fractionation vectors, calculated from mineral compositions in McKenzie and O'Nions (1991), are identified as follows: ol—olivine; opx—orthopyroxene; cpx—clinopyroxene; pl—plagioclase (An 80); hb—hornblende. Experimental mantle melts (A) and (B) for fluid present (Hy—half squares) and anhydrous and dehydration melts (An—asterisks) of peridotite KLB-1 at 1.0 GPa are from Hirose (1997 and references cited therein); experimental temperatures are indicated. The hachured field is the range of N-MORB basalts and associated fractionates from the Lower Cajul Formation (LCAJ), southwest Puerto Rico (Fig. 2A, Sierra Bermeja area), which represents the pre-arc basement.

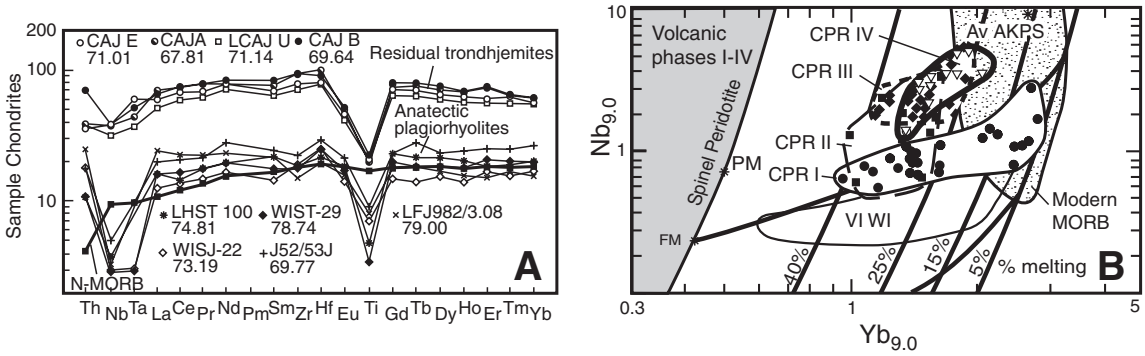

Figure 6. (A) Top—Chondrite-normalized patterns of pre-arc trondhjemites (Fig. 5A–B), representing residue of advanced fractional crystallization of MORB tholeiites (Jolly et al., 2006). Bottom—patterns of representative Antilles anatectic plagiorhyolites, including the Albian Water Island Formation (WI) and Cenomanian Louisenhoj Formation (LH) from the Virgin Islands, Lower Albian Formation J (J) from central Puerto Rico, and the Albian lower tuff of the Fajardo Formation (LFJ) from northeast Puerto Rico, compared with N-MORB (Sun and McDonough, 1989). SiO_2 content (wt %) is indicated beneath sample name. (B) Covariation of Nb_9 and Yb_9 in central Puerto Rican basalts (SiO_2 <55%), normalized to MgO = 9.0% (Pearce and Parkinson, 1993); volcanic phases are as in Figure 5; also included is the Water Island Formation from the Virgin Islands (VIWI), a correlative of volcanic phase I in central Puerto Rico. Melting track for FM is from Pearce and Parkinson (1993); PM represents the primitive mantle of Sun and McDonough (1989); modern (Atlantic) MORB is from Dosso et al. (1993); AKPS, Atlantic Cretaceous pelagic sediment. Puerto Rican data concentrate between the 22% and 40% melting contours.

higher SiO_2, indicating the two suites had different starting compositions. Both suites are represented in all volcanic phases in central Puerto Rico (Fig. 5), but high-Fe island arc tholeiite basalts dominate initial Albian strata (phases I and II), whereas low-Fe andesites dominate subsequent Cenomanian and Campanian strata (phase III). Similar proportions of the two suites are reported elsewhere in the Greater Antilles, where high-Fe island arc tholeiite basalts (or primitive island arc basalts in the terminology of Donnelly and Rogers, 1980) dominate Albian sequences, and low-Fe andesites tend to dominate post-Albian sequences (see, for example, Kesler et al., 2005; Pindell et al., 2006). Mafic end members of tholeiitic units partly overlap the field of anhydrous mantle melts (Hirose, 1997 and references cited therein) in the SiO_2 versus FeO*/MgO plot, whereas more siliceous low-Fe units partly overlap compositions of fluid-present mantle melts (Fig. 5A). Al_2O_3 content of the high-Fe suite decreases from a maximum of ~18% in volcanic phase I (Formation A, Fig. 5D) to a minimum of between 12% and 14% in phase III (Perchas basalts, Fig. 5H).

Plagiorhyolites

In addition to being the most siliceous rocks in central Puerto Rico, the dacite and rhyolite end members from volcanic phase I (Formation J2, Fig. 5D) are highly depleted in Al_2O_3 (12%–16%) and K_2O (<1.5%, Appendix Table 3), and have low $(Sr/Yb)_N$ (<1.0) compared with other felsic units. These features, together with relatively flat, normalized, incompatible element patterns (Appendix Figure 2D) and the ubiquitous presence of plagioclase, are hallmarks of the crustally derived intrusive plagiogranite series of Coleman and Peterman (1975; see also Coleman and Donato, 1979), which is a common, small-volume leucocratic vein component in Cenozoic oceanic crust (Coleman and Peterman, 1975; Flagler and Spray, 1991; Floyd et al., 1998; Koepke et al., 2004, 2007) and in ancient ophiolite settings (Coleman and Donato, 1979; Pallister and Knight, 1981; Alabaster et al., 1982; Floyd et al., 1998; Jolly and Lidiak, 2006; Dilek and Thy, 2006). Plagiorhyolites, the extrusive counterparts (Tsvetkov, 1991), normally comprise felsic end members of basalt-dominated bimodal suites in early strata from Cenozoic island arcs (Koepke et al., 2004), including the Cascades (Gerlach et al., 1981), Aleutians (Tsevtkov, 1991), Izu-Bonin (Tamura and Tatsumi, 2002), and Tonga-Kermadec (Smith et al., 2003). Plagiorhyolite is also present in Phanerozoic arcs, such as the Urals (Yazeva, 1978) and the Bay of Islands, Newfoundland (Malpas, 1979). Sometimes utilized to designate veins with adakite compositions characteristic of high-pressure slab melts with high SiO_2, Al_2O_3 >15%, Na_2O, Sr/Y <10, and La/Sm, and a fractionated normalized HREE pattern with low Yb (Kepezhinskas et al., 1995; Drummond et al., 1996; Luchitskaya et al., 2005), the term plagiorhyolite is restricted here to plagiophyric lavas with low K_2O <1.5%, Al_2O_3 <15%, Sr/Y <10, and REE, and relatively flat, normalized REE patterns.

Trace-Element Geochemistry

Basalts and Andesites

The concentration of Yb in mantle basalts is controlled mainly by the degree of fusion in a garnet-free peridotite source, while Nb abundance is proportional to both relative degree of incompatible element enrichment of the source and degree of melting. Consequently, covariation of these elements, when normalized to a standardized MgO content of 9% (SiO_2 <55%), provides estimates of both source composition and degree of melting in island arc settings. For this purpose, Pearce and Parkinson (1993) constructed a $(Yb\text{-}Nb)_9$ melting grid from calculated spinel peridotite melting curves and associated contours representing 40%, 25%, 15%, and 5% fractional melting of the mantle sources (Fig. 6B). The field of the Water Island Formation in the Virgin Islands (Jolly et al., 2006), the most depleted unit in the northeast Antilles, plots below the melting trajectory of the fertile MORB mantle (FM), consistent with a slightly depleted source composition. For the present purposes, the source is inferred to have consisted of the residue of a 2% melt of an FM-type source (RM2; Jolly et al., 2006). Concentrations of Nb_9 increase from 0.5 to over 5 ppm between volcanic phases I and IV in central Puerto Rico, consistent with a gradual increase in the degree of incompatible element source enrichment. There is a comparatively narrow range in Yb_9 from 0.8 to 1.5 ppm, such that most samples from all volcanic phases are concentrated in a band between the 20% and

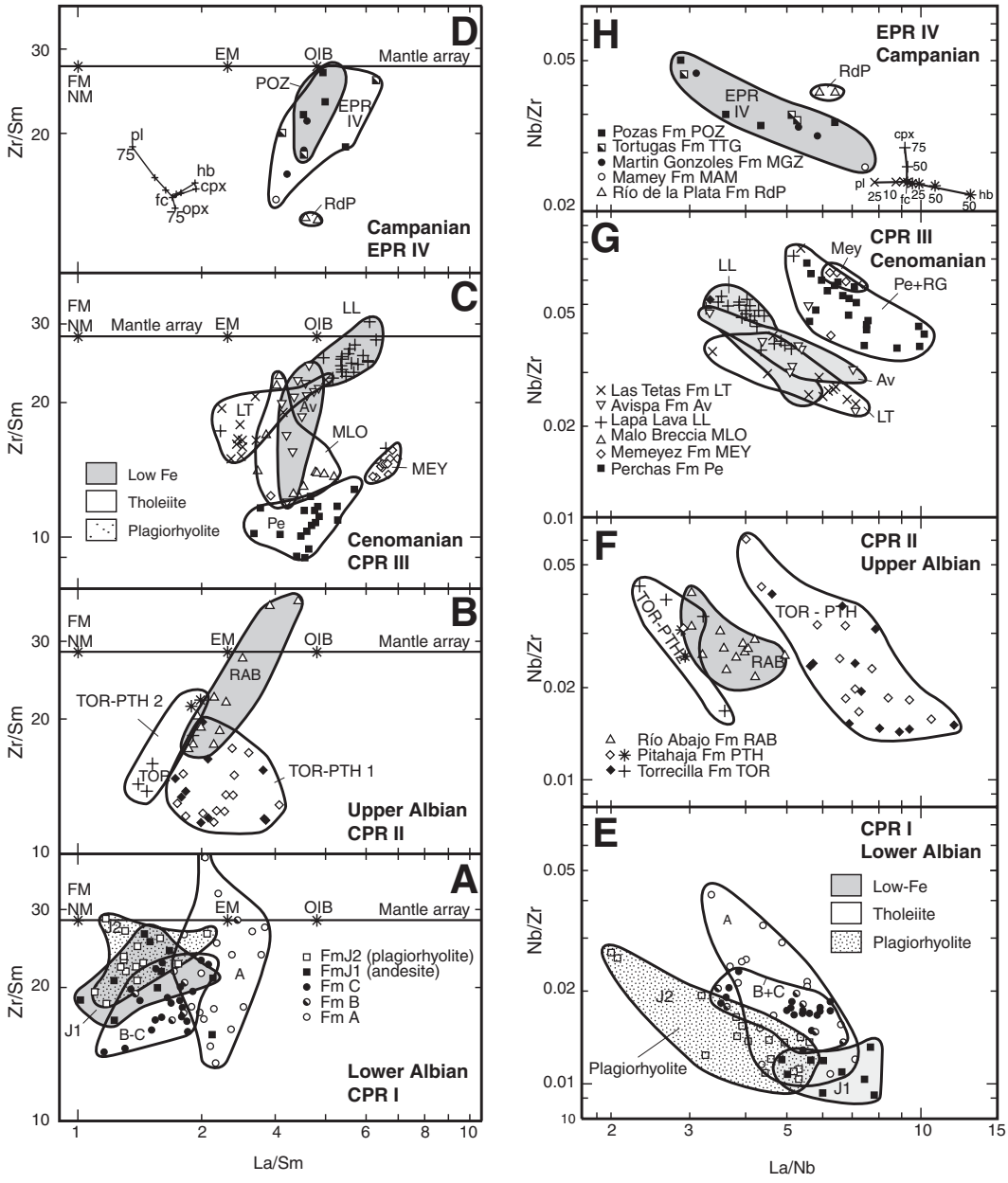

Figure 7. (A–D) La/Sm-Zr/Sm and (E–H) La/Nb-Nb/Zr in lavas from central Puerto Rico. Low-Fe units (shaded) have elevated Zr/Sm compared with high-Fe island arc tholeiites. Note that the field of Formations B and C is offset and subparallel to plagiorhyolites from Formation J, consistent with crustal contamination. Fractional crystallization vectors (fc) are as in Figure 11; mantle components are as in Figure 4.

40% melting contours, with a few as low as 5%. A value of 25% melting is adopted for use in mantle models presented in this paper.

Major features of the rocks are revealed in binary plots involving La/Sm and Zr/Sm, which reflect relative normalized LREE slopes and the magnitude of Zr anomalies, respectively (Fig. 7A–D). In high-Fe island arc tholeiites, there is a gradual decrease in Zr/Sm (reflecting deepening normalized Zr anomalies) and an increase in La/Sm (reflecting increasing source enrichment) with decreasing age. For instance, Zr/Sm decreases from between 15 and ~30 in volcanic phase I, to between 12 and 25 in phase II, and finally to minimum values of between ~10–20 in phases III and IV (Fig. 7A), whereas La/Sm increases from between 1 and 3 in phase I, to between 1.5 and 3 in phase II, to between 2 and 5 in phase III. In comparison, low-Fe units have slightly more elevated La/Sm and Zr/Sm. Like La/Sm, Nb/Zr increases from between 0.01 and 0.03 in volcanic phase I to as much as 0.08 in phase III. The variations are too large to represent fractional crystallization or accumulation of phenocrysts, and more likely reflect the presence of a high La/Sm-Zr/Sm component in low-Fe units. The Malo Breccia and andesites from the Avispa Formation bridge the gap between Perchas-type low-Zr/Sm and Lapa Lava-type high-La/Sm samples, indicating possible magma mixing (Fig. 7C). Low-Fe units have lower La/Nb (shallower normalized negative Nb anomalies) in any given volcanic phase compared with high-Fe island arc tholeiites (Fig. 7E–H).

Plagiorhyolite

Two separate, low-pressure plagiorhyolite series are recognized (Coleman and Donato, 1979; Malpas, 1979; Gerlach et al., 1981; Floyd et al., 1998; Koepke et al., 2004). They are difficult to distinguish from major-element data (Koepke et al., 2007), but are readily subdivided from normalized REE spectra (bottom of Fig. 6A) into (1) a high-REE, fractional crystallization-related

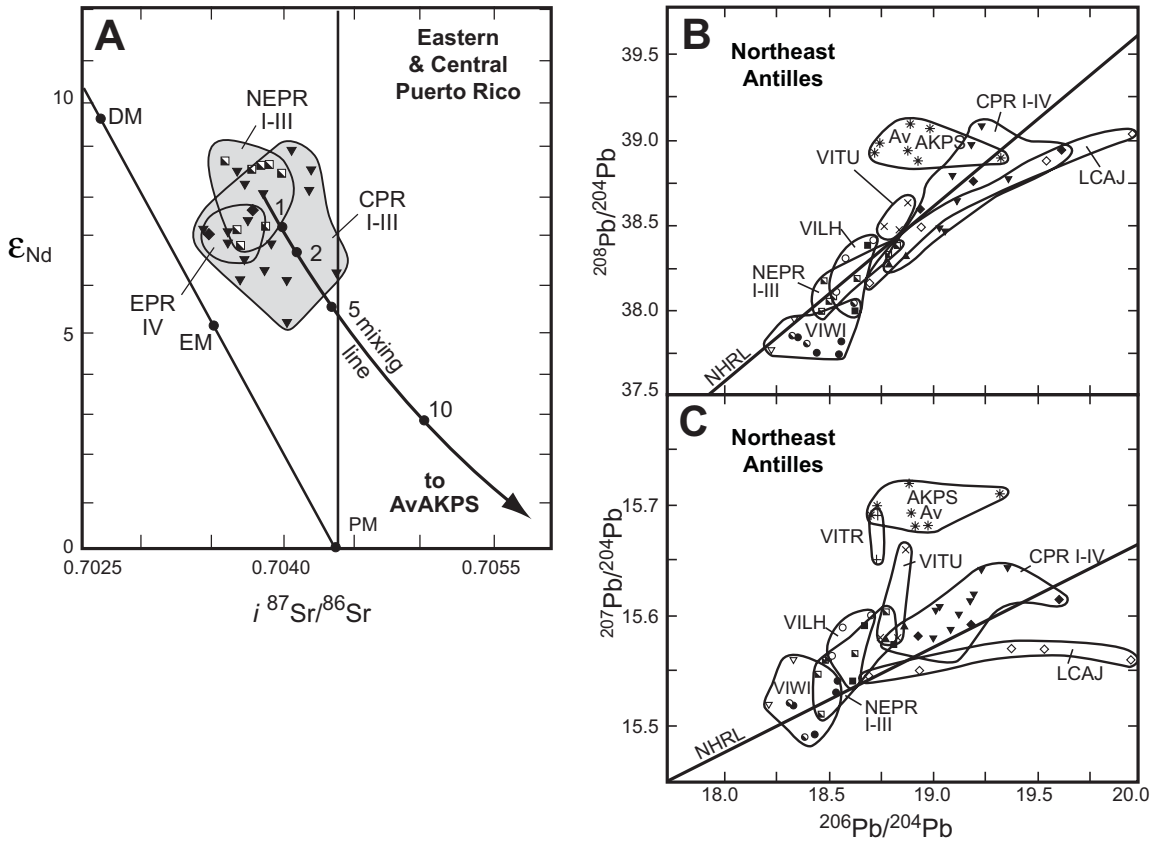

Figure 8. Sr, Nd, and Pb isotope ratios in the northeast Antilles; mantle features are from Rollinson (1993); DM—depleted N-MORB–type mantle; EM—E-MORB–type mantle. (A) Sr and Nd isotope ratios of island arc lavas from northeast (NERP I–III, EPR IV) and central (CPR I–III) Puerto Rico; volcanic phases are as in Figure 5. The mixing line between a sediment-poor sample from Formation A in central Puerto Rico and average Atlantic Cretaceous pelagic sediment (AKPS) is from Jolly et al. (2001). (B)–(C) $^{206}Pb/^{204}Pb$, $^{207}Pb/^{204}Pb$, and $^{208}Pb/^{204}Pb$ ratios in the northeast Antilles compiled from Frost et al. (1998) and Jolly et al. (1998, 2001, 2006, and Virgin Islands unpublished data). Virgin Islands units identified as follows (Rankin, 2002): VIWI—Albian Water Island Formation; VILH—Cenomanian Louisenhoj Formation; VITU—Santonian to Campanian Tutu Formation; LCAJ—Lower Cajul Formation, southwest Puerto Rico. The northern hemisphere reference line (NHRL) is from Hart (1984).

(residual) series, and (2) a low-REE, crustal melting-related (anatectic) series. There is a small range in LREE slopes in Antilles plagiorhyolites, from slightly depleted in early types, such as the Water Island Formation in the Virgin Islands (Jolly and Lidiak, 2006) to slightly enriched in later units (Fig. 6A), such as Formation J from volcanic phase I (Fig. 2B) in central Puerto Rico. The comparatively low-LREE concentrations in all Antilles varieties are characteristic of the anatectic plagiorhyolite variety.

Sr, Nd, and Pb Isotope Geochemistry

Initial Nd-Sr isotope ratios of Antilles Island Arc lavas form an elongate cluster subparallel to but offset toward elevated $i^{87}Sr/^{86}Sr$, consistent with seafloor alteration similar to that observed in Atlantic Cretaceous MORB (Jahn et al., 1980). ε_{Nd} ranges from ~8.5–6.5, while $i^{87}Sr/^{86}Sr$ (Fig. 8A) has a range from 0.7035 to 0.7044. An estimate of the proportion of Atlantic pelagic sediment required to produce the observed range of lavas is obtained from a calculated mixing line with end members that include (1) the inversion source (f = 0.25) of a phase I (CPR I) basalt (sample A-5 from Formation A; Jolly et al., 2001) and (2) the average AKPS composition. The position of the Puerto Rican field along the mixing curve is consistent with the presence of up to 4% sediment, similar to maximum levels in modern arcs (Ellam et al., 1988; Ellam and Hawkesworth, 1988). This is a minimum estimate, since it does not include the sediment component of the starting basalt.

Pb isotope ratios (Fig. 8B–C; Appendix Table 2) cluster subparallel to the northern hemisphere reference line (NHRL; Hart, 1984). $^{206}Pb/^{204}Pb$ increases gradually from depleted MORB-like values (18.3–18.4) in the Virgin Islands, to between 18.5–19.0 in northeast Puerto Rico, and finally to elevated levels ranging from 18.8 to over 19.5 in central Puerto Rico. This distribution is consistent with eastward decrease in the proportion of a U-Pb–enriched high μ (HIMU) component (Hart, 1984) in the mantle wedge source (Jolly et al., 2006). Superimposed on this compositional shift are additional variations of $^{207}Pb/^{204}Pb$ and $^{208}Pb/^{204}Pb$, consistent with introduction of variable proportions of incompatible element-enriched pelagic sediment with elevated radiogenic Pb. Jolly et al. (2006) reported that basalts and plagiorhyolites from the Water Island formation in the Virgin Islands have overlapping isotopic ratios with narrow ranges of $Pb\Delta^{8}/_{4}$ (averaging approximately −5), $i^{87}Sr/^{86}Sr$ (0.7035–0.7040), and ε_{Nd} (from 7 to 10).

MELTING MODELS

Three melting models are evaluated in the following sections, including (1) high-pressure partial fusion of spinel peridotite; (2) high-pressure, high-degree fusion of the two pelagic sediment end members present in Atlantic Cretaceous sediment, biogenic sediment, and turbidite detritus of upper continental crust composition; and (3) low-pressure partial melting of amphibole-bearing gabbro of N-MORB–type oceanic crust composition. In addition, mixing models involving the inferred mantle wedge source and various proportions of melts derived from the subducted sediment component are assessed.

Mantle Wedge Component

The spinel lherzolite adopted for use in mantle melting models consists of 57.5% olivine (ol), 27.0% orthopyroxene (opx), 12.5% clinopyroxene (cpx), and 3.0% spinel (McKenzie and O'Nions, 1991). Amphibole is not included because it is absent in high-pressure experimental peridotite melts under hydrous conditions (Hirose, 1997). It is inferred (1) that cpx disappears after 25% melting, opx after 40%, and spinel after 80% (Pearce and Parkinson, 1993), and (2) that phases disappear from the source at constant rates, such that orthopyroxene is converted to olivine during early stages of fusion. REE partition coefficients (D-values) for fractional melting of spinel peridotite and fractional crystallization of basaltic melts are adopted from the set compiled by Pearce and Parkinson (1993) and modified by Bédard (1999). The mixing models illustrated in Figures 9 through 12 are all based on 25% melts (f = 0.25) of a residual (RM2) peridotite wedge source following extraction of a 2% melt (Fig. 6B). However, because incompatible element ratios of sources are similar to melts at such high degrees of fusion, results are virtually identical in plots involving raw source mixtures.

Pelagic Sediment Component

The presence of well-developed, negative normalized HFSE anomalies in Antilles high-Fe arc basalts of all ages (Fig. 3C–E) tends naturally to favor a persistent south-dipping subduction model, because the patterns closely resemble biogenic clays and carbonates from Atlantic Cretaceous pelagic sediment. In contrast, the relatively pure and highly refractory pelagic chert in the Pacific basin has flat to strongly positive Nb anomalies inconsistent with patterns of the high-Fe Antilles island arc tholeiite suite. Since Nichols et al. (1994) and Tatsumi (2001) demonstrated that subducted pelagic sediments can melt at the high-temperature, high-pressure conditions expected in the upper part of the descending slab, it is possible to evaluate the role of Atlantic sediments from trace-element equilibrium batch melting models (Shaw, 1970). Parameters adopted for the models are based on the experiments of Tatsumi, in which between 50% and 75% melting (f = 0.5–0.75) was required to generate appropriate melt compositions in a process that produced residua consisting of garnet (40%), quartz (40%), and sillimanite (20%); residual oxide phases were absent, as expected at such high degrees of melting (Ryerson and Watson, 1987). D-values are interpolated from values of Tatsumi, and for consistency it is inferred that D-values remain constant for all sediment compositions. At least two different trends are possible for melts in equilibrium with a garnet-quartz-sillimanite residual assemblage, depending on the selection of REE distribution coefficients for garnet. Behavior of HFSE and REE are normally regarded as incompatible (see, for example, McKenzie and O'Nions, 1991), such that progressive equilibrium batch melting produces melts with relatively constant incompatible element ratios at high degrees of melting (>50%; Tatsumi, 2001). If HFSE are compatible with respect to REE in garnet, as suggested by van Westrenen et al. (2001), then Zr/Sm decreases significantly with decreasing degree of melting. During this work, it was determined that treating Zr as a compatible component, with a D-value between 1 and 3, produces abnormally low Zr/Sm. Conversely, treating Zr as incompatible, with a D-value of 0.3 (McKenzie and O'Nions, 1991), produces better results in accord with observed compositions.

Two-Component (Mantle Source and Biogenic Pelagic Sediment) Mixing Models

Although a broad range of Zr/Sm is represented in Cretaceous pelagic sediment from the Atlantic Ocean (AKPS; Fig. 3A), low Zr/Sm biogenic oceanic platform deposits dominated pelagic sedimentation in the Atlantic basin during the Cretaceous (Fig. 4C). This setting is consistent with the general resemblance between normalized, incompatible element spectra of Puerto Rican high-Fe arc tholeiites (Fig. 3D; Appendix Fig. 2) and biogenic end members from the Atlantic sediment reservoir, such as sample 417D/19/1 (Fig. 3A). Estimates of the proportion of sediment incorporated by the tholeiites are most reliably derived from two-component mixing models. For instance, the track of a mixing line produced by 25% melting in a series of RM2 sources containing 0.5%, 1%, 2%, 4%, 6%, 8%, and 10% biogenic sediment (Fig. 9A–B) is subparallel to fields of high-Fe units in La/Sm versus Zr/Sm and La/Nb and Nb/Zr plots (Figs. 9C and 9D, respectively), consistent with incorporation of increasing proportions of biogenic sediment. The concurrent decrease in Zr/Sm from oldest to youngest tholeiitic units reflects increasing proportions of biogenic sediment, ranging from between 0.5% and 1% in phase I, to ~1% in phase II, and finally to between 2% and 4% in phase III. These estimates are consistent with chondrite-normalized incompatible element spectra, which reproduce both negative HFSE anomalies and REE slopes

Figure 9. Covariation of La/Sm versus Zr/Sm and La/Nb versus Nb/Zr in arc lavas from the northeast Antilles; similar plots for La/Nb versus Nb/Zr in northeast Puerto Rico and the Virgin Islands are given in Jolly et al. (2006). (A) and (B) Key to petrogenetic models, including melting tracks (f = 0.25, 0.50, 0.75) for two pelagic sediment end members: (1) the most biogenic Atlantic Cretaceous pelagic sediment (sample DSDP 417D/19/1, Jolly et al., 2006) and (2) the average upper continental crust (UCC; Plank and Langmuir, 1998). Also shown are mixing lines between an RM2-type source (equivalent to an N-MORB–type peridotite source following removal of a 2% melt fraction, Pearce and Parkinson, 1993) and various proportions (0.5%, 1%, 2%, 4%, 6%, 8%, and 10%) of sediment melt (f = 0.5) derived from the two sediment end members, and an associated mixing grid. Also indicated are: (A) fields of expected island arc melt compositions; (B) fractional crystallization vectors for plagioclase (pl), hornblende (hb), and clinopyroxene (cpx), which were calculated from partition coefficients of McKenzie and O'Nions (1991); (C) the array of Atlantic pelagic sediment (AKPS) compositions; and (D) the mantle array (codes as in Fig. 11). (C) and (D) Compositions of high-Fe island arc tholeiite basalts compared to mixing track between RM2-type source and biogenic sediment melt. (E) and (F) Compositions of low-Fe andesites units superimposed on a grid representing mixing between an RM2-type source (representing an N-MORB–type source following extraction of a 2% melt fraction) and melts (f = 0.5) derived from the two sediment end members (biogenic and upper continental crust).

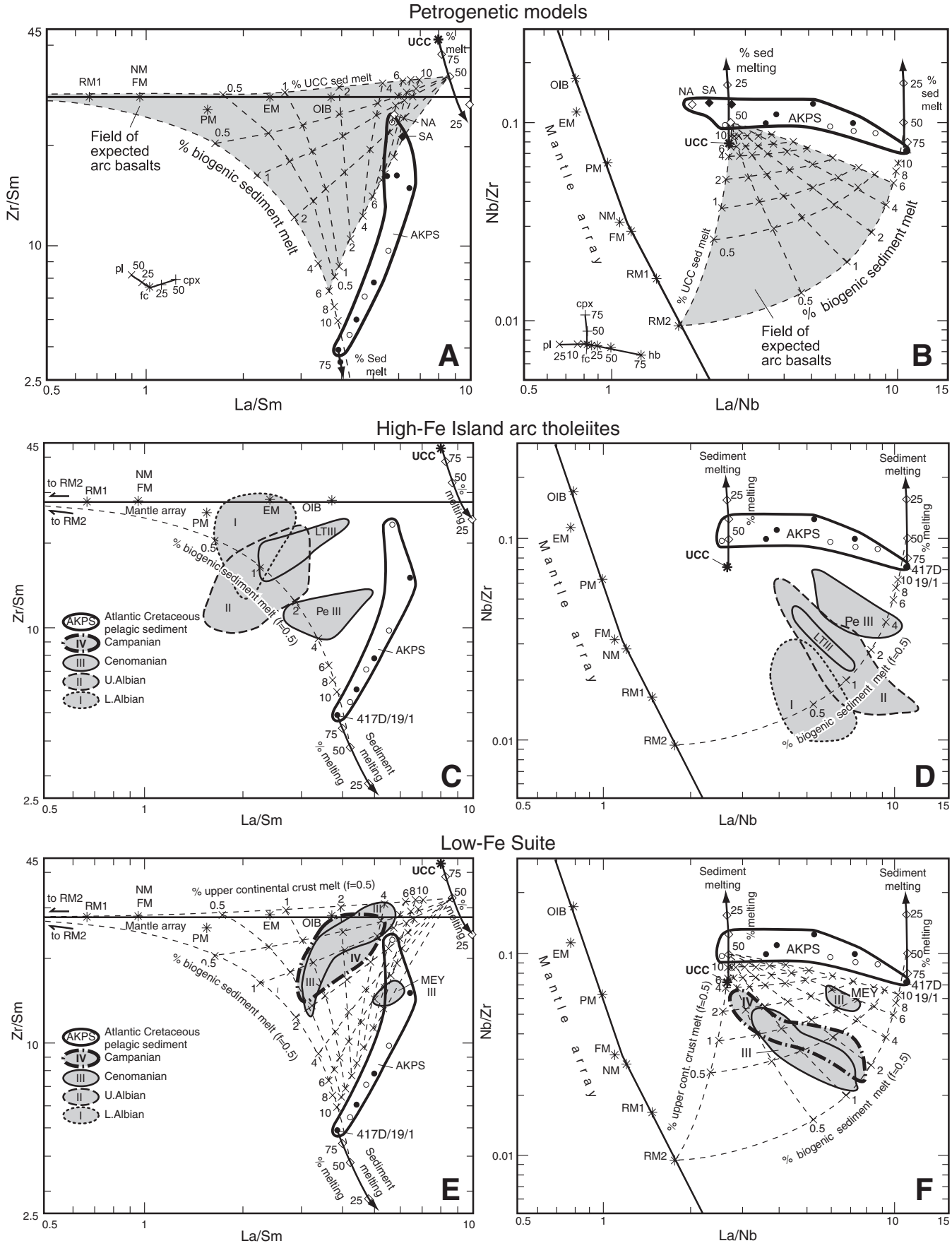
Petrogenetic models
Zr/Sm
La/Sm
Nb/Zr
La/Nb
UCC
RM1
NM
FM
PM
EM
OIB
NA
SA
AKPS
Field of expected arc basalts
% biogenic sediment melt
% UCC sed melt
% Sed melt
% sed melting
% biogenic sediment melt
Mantle array
RM2
pl
cpx
fc
hb
A
B
High-Fe Island arc tholeiites
to RM2
Mantle array
I
II
LTIII
Pe III
417D/19/1
% biogenic sediment melt (f=0.5)
Atlantic Cretaceous pelagic sediment
Campanian
Cenomanian
U.Albian
L.Albian
% melting
Sediment melting
C
D
Low-Fe Suite
% upper continental crust melt (f=0.5)
MEY
% upper cont. crust melt (f=0.5)
E
F

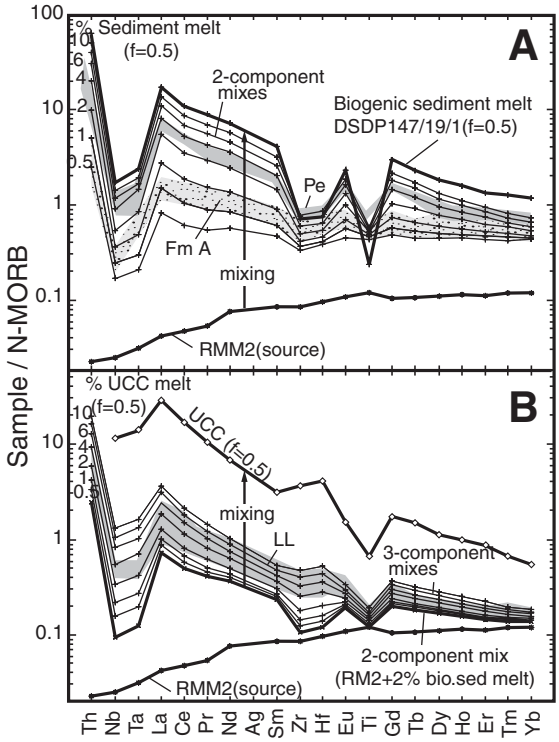

Figure 10. N-MORB–normalized incompatible element patterns of selected central Puerto Rico lavas compared with calculated mixing models. Proportions of sediment melt (f = 0.5) added to the calculated mixes are indicated at left. (A) Fields of Formation A from volcanic phase I and the Perchas Formation (Pe) from phase III are superimposed on patterns generated by mixes involving various proportions (0.5%, 1%, 2%, 4%, 6%, 8%, and 10%) of biogenic sediment sample 417D/19/1 and an RM2-type source. (B) Field of Lapa Lava (LL) from phase III is superimposed on three-component mixing models between an RM2-type source containing a 2% melt fraction (f = 0.5) derived from high-pressure fusion of biogenic sediment, together with various proportions of melt (f = 0.5) derived from turbidites of upper continental crust origin. Partition coefficients, some interpolated, during slab melting for garnet (modified from Tatsumi, 2001) include the following: Th, 0.001; Nb and Ta, 0.01; La, 0.010; Ce, 0.210; Pr, 0.0548; Nd, 0.087; Sm, 0.217; Zr and Hf, 0.3; Eu, 3.2; Ti, 150; Gd, 0.50; Dr, 1.06; Er, 2.0; Yb, 4.08; references are given in text.

characteristic of high-Fe tholeiites. For example, patterns of low-La basalts from Formation A (volcanic phase I) overlap mixtures with 0.5%–2% of melt generated by melting (f = 0.5) of biogenic sediment, whereas high-La Perchas basalts (phase III) overlap mixes containing 4%–6% biogenic sediment melt (Fig. 10A).

Upper Continental Crust Component

Simple two-component models do not reproduce the much shallower negative normalized Nb and Zr anomalies typical of members of the low-Fe Antilles suite, such as the Lapa Lava (Fig. 3C). Instead, higher Zr/Sm and lower La/Nb values in these rocks more closely resemble high-pressure slab melts, basalts from the mantle array, and continental crust. Antilles arc lavas probably did not incorporate slab melts, since that would require maintenance of anomalously elevated geothermal gradients in the subducting plate for extended periods of time (Defant and Drummond, 1990; Rapp et al., 1999). Moreover, because La/Sm of several low-Fe units significantly exceed values of OIB, it is unlikely that the observed compositions were produced by an enriched mantle component. Instead, the variations more likely reflect incorporation of upper continental crust (UCC) detritus of turbiditic origin, a mechanism also proposed to explain elevated Pb-isotope ratios in arc rocks of similar age and geologic setting from eastern Cuba (Marchesi et al., 2007). To assess this process, a three-component mixing grid is required (Figs. 9A–B and 9E–F), incorporating not only (1) the RM2 source and (2) a biogenic sediment end member, but also (3) the average UCC (Plank and Langmuir, 1998). The fields of low-Fe units on the resulting grid (Fig. 9E–F) converge on the composition of melt derived from fusion (f = 0.5) of UCC. The results are consistent with incorporation of up to 2% crustal sediment melt in addition to 0.5%–2% biogenic sediment. They are also consistent with normalized incompatible element patterns of the calculated mixtures, which overlap low-Fe units, reproducing the characteristic shallow negative Zr anomalies and relatively steep LREE slopes (Fig. 10B).

Anatectic Plagiorhyolite Component

Experimental studies, mostly at 1 atm in dry basalt systems, reveal that fractional crystallization of clinopyroxene-plagioclase-Fe-Ti-oxide–rich assemblages from a basaltic parent produces residual plagiorhyolite compositions with elevated incompatible element concentrations (Juster et al., 1989; Thy and Lofgren, 1994; Toplis and Carroll, 1995). In contrast, fusion of wet gabbro at crustal pressures (Baker and Eggler, 1987; Housh and Luhr, 1991; Beard, 1995; Koepke et al., 2004) generates both plagiorhyolite and higher degree andesite melts with comparatively low incompatible element concentrations, similar to Antilles plagiorhyolites (Fig. 6A). For example, Koepke et al. (2004) produced low-K andesitic compositions by ~15% melting at 200 MPa and temperatures between 900º and 940º C, leaving residues of plagioclase + clinopyroxene + amphibole. Low-Ti starting material precluded involvement of Ti-Nb oxide phases, but other authors (Ryerson and Watson, 1987; Hirose, 1997) reported residual Ti-bearing opaque phases following water-present fusion of peridotite at pressures of 1 KPa, consistent with characteristic well-developed, negative normalized Ti and Nb anomalies.

Crustal fusion induced by ascent of mantle-derived melts is most likely to occur in the lower crust, where temperatures are higher and layered gabbros and associated accumulates predominate (cf. Floyd et al., 1998). Accordingly, crustal anatexis models, calculated utilizing the Shaw (1970) equation for modal equilibrium batch melting and partition coefficients from McKenzie and O'Nions (1991), are evaluated for two different types of altered basaltic crust, amphibole gabbro and amphibolite (Fig. 11A–B). An amphibolite with MORB-like compositions from the pre-arc basement complex in western Puerto Rico was selected as starting composition (sample AMPH30, Jolly and Lidiak, 2006). When cast as an amphibole gabbro source (model 1), consisting of a 45:39:15:1 augite-plagioclase-hornblende-magnetite mixture (Fig. 11A), melting produces a series of slightly depleted, chondrite-normalized REE patterns (f – 0.5, 0.25, 0.15, 0.05 indicated by "+" symbols and thin

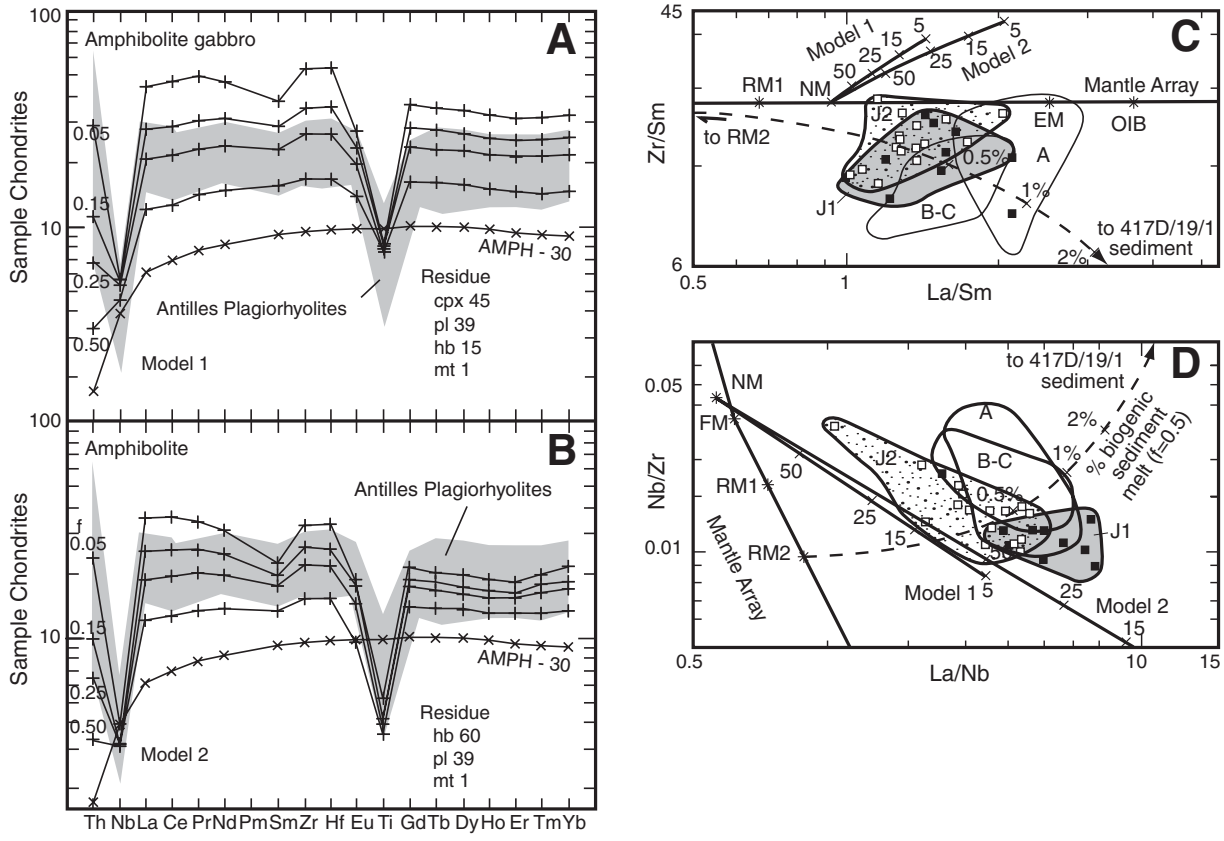

Figure 11. (A) and (B) Low-pressure melting models 1 and 2, representing generation of plagiorhyolite melts through fusion of an N-MORB–like, amphibole-bearing gabbroic parent (sample AMPH-30), leaving residues of 45% clinopyroxene, 39% plagioclase, 15% hornblende, and 1% magnetite (amphibole gabbro model 1) and 60% hornblende, 39% plagioclase, and 1% magnetite (amphibolite model 2), respectively. Model melts of various degrees of melting (f = 0.5, 0.25, 0.15, 0.05) are indicated by solid lines and "+" symbols. (C) and (D) Covariation of La/Sm-Zr/Sm and La/Nb-Nb/Zr in Early Albian lavas from central Puerto Rico. Units are identified as follows: J1—plagiorhyolite from Formation J; J2—andesite; A, B, C—Formation A, B, and C. Melting tracks for low-pressure equilibrium batch melting of N-MORB–type amphibole gabbro (Model 1) and amphibolite (Model 2) are also included. Atlantic Cretaceous pelagic sediments (AKPS) are from Jolly et al. (2006). Symbols are as follows: FM—fertile MORB mantle (Pearce and Parkinson, 1993; Bédard, 1999); RM1—residual MORB mantle from 1% melt. Normal MORB (NM), enriched MORB (EM), and ocean island basalt (OIB) are from Sun and McDonough (1989).

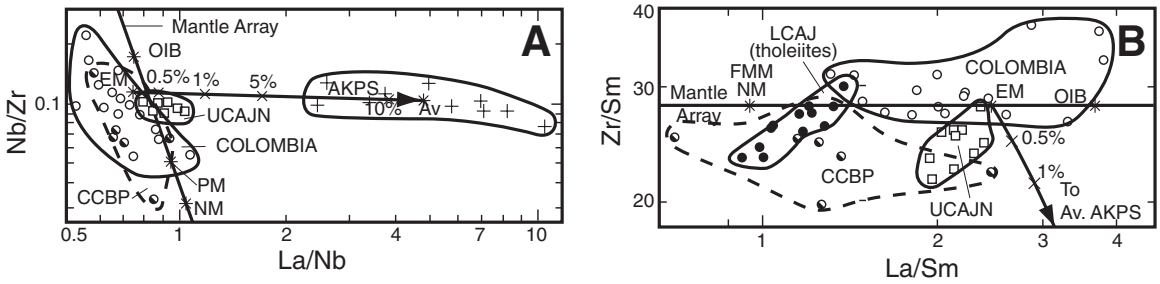

Figure 12. (A) Covariation of La/Nb and Nb/Zr in the Caribbean Cretaceous plateau basalts. Samples are from the Colombian basalt plateau (Kerr et al., 2002), the central Caribbean basalt plateau (CCBP and DSDP samples from Jolly and Lidiak, 2006), and the northern sequence of the Upper Cajul Formation in southwest Puerto Rico (UCAJN). Also included is a calculated mixing line between E-MORB and the average Atlantic Cretaceous pelagic sediments. (B) La/Sm and Zr/Sm in Caribbean plateau lavas (symbols and mixing line as in A). Jurassic MORB tholeiites (LCAJ) from the pre-arc basement in southwest Puerto Rico (modified from Jolly and Lidiak, 2006) are included; mixing line as in A.

lines in Fig. 11A–B) that, at between 15%–50% melting, resemble Antilles plagiorhyolites. The patterns include small negative Eu anomalies, deep negative Nb and Ti anomalies (consistent with fractional crystallization of Ti-bearing oxide phases), and slightly positive Zr anomalies. An alternative amphibolite source (model 2), representing strongly hydrated gabbro consisting of a 60:39:1 hornblende-plagioclase-magnetite mixture (Fig. 11B), produces melts, with similar patterns with slightly more enriched normalized LREE slopes at relatively low degrees of melting (15%–25%), which also overlap the Antilles plagiorhyolite suite.

Calculated trajectories for equilibrium batch melting of altered oceanic crust with N-MORB–type (NM) trace-element composition trajectories for models 1 and 2 on La/Sm versus Zr/Sm and La/Nb versus Nb/Zr are illustrated in Figure 11C–D. Fields for plagiorhyolites (stippled) and andesites (shaded) from Formation J, as well as fields for associated Lower Albian Formations A, B, and C, lie off the predicted melting paths in both plots. However, since most fields are subparallel to the melting curves and are offset consistently toward biogenic pelagic sediments, compositions are consistent with remelting of underplated arc-related crust. Fields of formation J plagiorhyolites and andesites intersect the source-sediment mixing curve at slightly <0.5% sediment compared with between 0.5% and 1.0% for Formations B + C. The diagonal field of Formation A is consistent with a more variable crustal component. The excess energy required for voluminous melting of sub-arc oceanic crust in northeast Puerto Rico is inferred to have been supplied by repeated ascent of high-temperature island arc melts from mantle depths. Anomalous heating may also reflect proximity to the subducting, still-spreading, mid-Atlantic ridge (Fig. 1B, Jolly and Lidiak, 2006; Pindell et al., 2006).

TECTONIC IMPLICATIONS

Suprasubduction Zone Component

Several lines of evidence indicate that sediments subducted during Cretaceous island arc development in the northeast Antilles originated in the restricted southwest spur of the North Atlantic Ocean. First, Cretaceous pelagic sediments from the Atlantic basin are dominated by biogenic sediments, carbonates, and continental detritus with N-MORB–normalized incompatible element spectra, including negative Nb and variable Zr anomalies, that closely match patterns of arc lavas. In contrast, sediments from the open Pacific Ocean consisted predominantly of radiolarian chert with low incompatible element content, and with normalized patterns characterized by positive Nb anomalies. Because the older southwest-dipping subduction zone in northeast Puerto Rico had already been operative for at least 15 million years when the Caribbean basalt plateau was erupted (92–88 Ma; Révillon et al., 2000), emplacement of the associated Caribbean mantle plume must have occurred within the broad back-arc region (suprasubduction zone) of the older, presumably southwest-dipping arc. In such a setting, permeating aqueous fluids and melts from the underlying Benioff zone are expected to overprint the upper mantle with a signature, most prominently characterized by negative normalized HFSE anomalies (Taylor and Martinez, 2003), Consequently, the absence of a suprasubduction zone component in Caribbean plateau basalts outside of Puerto Rico (Kerr et al., 2003), has favored island arc tectonic models involving northeast-dipping subduction (Lapierre et al., 1999; Révillon et al., 2000; Kerr and Tarney, 2005).

Detection of a suprasubduction zone component is inherently difficult in incompatible element-enriched rocks like the plateau basalts from southwestern Puerto Rico, because elevated trace-element and radiogenic isotope abundances in the enriched protolith dominate mixing proportions. The problem is simplified considerably in southwest Puerto Rico, because pelagic sediments in the Cretaceous Atlantic basin were dominated by high-REE and low-HFSE limestone and calcareous claystone (Fig. 4B; Donnelly, 1978). Accordingly, trace-element ratios provide markers of pelagic sediments originating in the Atlantic basin. For instance, La/Nb is significantly higher in plateau basalts from the Upper Cajul Formation (UCAJN in Fig. 12) than in Colombian counterparts. Moreover, the Puerto Rican plateau basalt field is offset in La/Nb-Nb/Zr plots (Fig. 12A) away from the mantle array and other mantle basalts toward AKPS, consistent with the presence of a small suprasubduction zone component of Atlantic origin. Similarly, Colombian plateau basalts concentrate above the mantle trend on La/Sm-Zr/Sm plots, whereas the fields of Puerto Rican and central Caribbean plateau basalts are significantly offset toward Atlantic sediment (Fig. 12B, Jolly et al., 2007). Relative to simple mixing lines between an inferred plume source (E-MORB Zr/Sm = 28; La/Nb = 0.75) and the average biogenic Atlantic sediment, compositions of Puerto Rican plateau basalts are consistent with a sediment content of ~0.5% (Fig. 12A–B).

CONCLUSIONS

Negative N-MORB–normalized Zr anomalies characteristic of high-Fe (island arc tholeiite) lavas from central Puerto Rico are inconsistent with northeast-dipping subduction of the chert-dominated Pacific (Farallon) Plate (Fig. 1B). Instead, the patterns reflect long-term, southwest-dipping subduction of low-Zr/Sm biogenic pelagic sediments of Atlantic origin, as in tectonic models like that proposed by Pindell and Barrett (1990) and Pindell et al. (2006) (Fig. 1C). Sr-Nd isotope and incompatible trace-element mixing models indicate that the proportion of biogenic sediment incorporated by high-Fe island arc tholeiites increased from less than 0.5% in Lower Albian volcanic phase I, to between 1% and 2% in Upper Albian phase II, and finally to ~4% in Cenomanian to Campanian phases III and IV, consistent with gradual accumulation of sediment on the subducting Atlantic floor. Members of the low-Fe suite, especially representatives from volcanic phases III and IV, are characterized by comparatively shallow normalized Zr anomalies. Models reproducing such patterns require incorporation not only of 1%–2% biogenic sediment, but also as much as 2% UCC, the latter of which was most likely contributed by turbidites originating from cratons bordering the Atlantic basin as the arc swept into the Caribbean slot (Fig. 1C). This conclusion is consistent with the presence of a low-Zr/Sm suprasubduction zone component of Atlantic origin in Caribbean plateau basalts (91–88 Ma) from southwest Puerto Rico, which were erupted within the broad backarc region of the Greater Antilles during intermediate stages of arc development.

ACKNOWLEDGMENTS

Reviews of the manuscript by Jean Bédard, John Lewis, and an anonymous reviewer, which substantially improved the presentation, are gratefully acknowledged. Financial support for this project is provided through Discovery Grants from the National Science and Engineering Council of Canada (NSERC). Graphics were prepared by M. Lozon of the Department of Earth Sciences, Brock University.

REFERENCES CITED

Alabaster, T., Pearce, J.A., and Malpas, J., 1982, The volcanic stratigraphy and petrogenesis of the Oman ophiolite: Contributions to Mineralogy and Petrology, v. 81, p. 168–183, doi: 10.1007/BF00371294.

Arculus, R.J., 2003, Use and abuse of the terms calcalkaline and calcalkalic: Journal of Petrology, v. 44, p. 929–935, doi: 10.1093/petrology/44.5.929.

Baker, D.R., and Eggler, D.H., 1987, Compositions of anhydrous and hydrous melts coexisting with plagioclase, augite, and olivine or low-Ca pyroxene from 1 atm to 8 kbar: Application to Aleutian volcanic center of Atka: The American Mineralogist, v. 72, p. 12–28.

Bawiec, W.J., 2001, Geology, geochemistry, geophysics, mineral occurrences, and mineral resource assessment for the Commonwealth of Puerto Rico: U.S. Geological Survey Open-File Report, CD ROM 98-38.

Beard, J.S., 1995, Experimental, geological, and geochemical constraints on the origins of low-K silicic magmas in oceanic arcs: Journal of Geophysical Research, v. 100, p. 15,593–15,600, doi: 10.1029/95JB00861.

Bédard, J.H., 1999, Petrogenesis of boninites from the Betts Cove Ophiolite, Newfoundland, Canada: Identification of subducted source components: Journal of Petrology, v. 40, no. 12, p. 1853–1889, doi: 10.1093/petrology/40.12.1853.

Briggs, R.P., 1969, Changes in stratigraphic nomenclature in the Cretaceous system, east-central Puerto Rico: U. S. Geological Survey Bulletin, 1274-O, 31 p.

Briggs, R.P., and Aguilar-Cortés, E., 1980, Geologic map of the Fajardo and Icacos: quadrangles, Puerto Rico: U.S. Geological Survey Miscellaneous Geologic Investigations Map I-1153.

Burke, K., 1988, Tectonic evolution of the Caribbean: Review of Earth and Planetary Sciences, v. 16, p. 210–230.

Coleman, R.G., and Donato, M.M., 1979, Oceanic plagiogranite revisited, *in* Barker, F., ed., Trondhjemites, dacites, and related rocks: Amsterdam-Oxford-New York, Elsevier, p. 149–167.

Coleman, R.G., and Peterman, Z., 1975, Oceanic plagiogranite: Journal of Geophysical Research, v. 80, p. 1099–1108.

Defant, M.J., and Drummond, M., 1990, Derivation of some modern arc magmas by melting of young subducted lithosphere: Nature, v. 347, p. 662–665, doi: 10.1038/347662a0.

Dilek, Y., and Thy, P., 2006, Age and petrogenesis of plagiogranite intrusions in the Ankara mélange, central Turkey: The Island Arc, v. 15, p. 44–57, doi: 10.1111/j.1440-1738.2006.00522.x.

Dolan, J., Mann, P., de Zoeten, R., Heubek, C., and Shiroma, J., 1991, Sedimentologic, stratigraphic, and tectonic synthesis of Eocene-Miocene sedimentary basins, Hispaniola and Puerto Rico: Geological Society of America Special Paper 262, p. 217–263.

Donnelly, T.W., 1978, Chemistry of sediments of the western Atlantic: Site 417 compared with sites 9, 105, 386, 387: Initial Reports of the Deep Sea Drilling Project, v. 51B53, p. 1515–1523.

Donnelly, T.W., 1989, Geologic history of the Caribbean and Central America: The geology of North America—An overview: Geological Society of America, The Geology of North America. V. A, p. 299–321.

Donnelly, T.W., and Rogers, J.J.W., 1980, Igneous series in island arcs: Bulletin of Volcanology, v. 43, p. 347–382, doi: 10.1007/BF02598038.

Donnelly, T.W., Thompson, G., and Salisbury, H., 1978, The chemistry of altered basalts at site 417, Leg 51: Initial Reports of the Deep Sea Drilling Project, v. 51–53, p. 1319–1330.

Dosso, L., Bougault, H., and Joron, J.-L., 1993, Geochemical morphology of the North Mid-Atlantic Ridge, 10-24°: Trace element-isotope complementarity: Earth and Planetary Science Letters, v. 120, p. 443–462, doi: 10.1016/0012-821X(93)90256-9.

Draper, G., Guitierrez, G., and Lewis, J.F., 1996, Thrust emplacement of the Hispaniola peridotite belt; orogenic expression of the mid-Cretaceous Caribbean arc polarity reversal?: Geology, v. 24, no. 12, p. 1143–1146.

Drummond, M.S., Defant, M.J., and Kepezhinski, P.K., 1996, Petrogenesis of slab-derived trondhjemite-tonalite-dacite/adakite magmas: Transactions of the Royal Society of Edinborough: Earth Sciences, v. 87, p. 205–215.

Ellam, R.M., and Hawkesworth, C.J., 1988, elemental and isotopic variations in subduction-related basalts: Evidence for a three component model: Contributions to Mineralogy and Petrology, v. 98, p. 72–80, doi: 10.1007/BF00371911.

Ellam, R.M., Menzies, M.A., Hawkesworth, C.J., Leeman, W.P., Rosi, M., and Serri, G., 1988, The transition from calc-alkaline to potassic orogenic magmatism in the Aeolian Islands, Southern Italy: Bulletin of Volcanology, v. 50, p. 386–398, doi: 10.1007/BF01050638.

Flagler, P.A., and Spray, J.G., 1991, Generation of plagiogranite by amphibolite anatexis in oceanic shear zones: Geology, v. 19, p. 70–73, doi: 10.1130/0091-7613(1991)019<0070:GOPBAA>2.3.CO;2.

Floyd, P.A., Yalinz, M.K., and Goncuoglu, M.C., 1998, Geochemistry and petrogenesis of intrusive and extrusive ophiolite plagiogranites: Central Anatolian Crystalline Complex, Turkey: Lithos, v. 42, p. 225–241, doi: 10.1016/S0024-4937(97)00044-3.

Frost, C.D., Schellekens, J. H., and Smith, A. L., 1998, Nd, Sr, and Pb isotope characterization of Cretaceous and Paleogene volcanic and plutonic island arc rocks from Puerto Rico: Geological Society of America Special Paper 322, p. 123–132.

Gerlach, D.C., Leeman, W.H., and Avé Lallement, H.G., 1981, Petrology and geochemistry of plagiogranite in the Canyon Mountain Ophiolite, Oregon: Contributions to Mineralogy and Petrology, v. 77, p. 82–92, doi: 10.1007/BF01161505.

Gill, J.B., 1981, Orogenic andesites and plate tectonics: Berlin, Springer-Verlag.

Gradstein, F.M., Ogg, J.G., and Smith, A.G., 2004, A geologic time scale: Cambridge, Cambridge University Press, 589 p.

Hart, S.R., 1984, A large-scale isotope anomaly in the southern hemisphere mantle: Nature, v. 309, p. 753–757, doi: 10.1038/309753a0.

Hauff, F., Hoernle, K., Tilton, G., Graham, D.W., and Kerr, A.C., 2000, Large volume recycling of oceanic lithosphere over short time scales: Geochemical constraints from the Caribbean Large Igneous Province: Earth and Planetary Science Letters, v. 174, p. 247–263, doi: 10.1016/S0012-821X(99)00272-1.

Hirose, K., 1997, Melting experiments on lherzolite KLB-1 under hydrous conditions and generation of high-magnesian andesitic melts: Geology, v. 25, p. 42–44, doi: 10.1130/0091-7613(1997)025<0042:MEOLKU>2.3.CO;2.

Housh, T.B., and Luhr, J.F., 1991, Plagioclase-melt equilibria in hydrous systems: American Mineralogist, v. 76, p. 477–492.

Iturralde-Vinent, M., Diaz-Otero, H., Rodriguez-Vega, A., and Diaz-Martinez, R., 2006, Tectonic implications of paleontologic dating of Cretaceous-Danian sections of eastern Cuba: Acta Geologica, v. 4, p. 89–102.

Jahn, B., Bernard-Griffiths, J., Charlot, R., Cornichet, J., and Vidal, F., 1980, Nd and Sr isotopic compositions and REE abundances of Cretaceous MORB (Holes 417D and 418A, Legs 51, 52, and 53): Earth and Planetary Science Letters, v. 48, p. 171–184, doi: 10.1016/0012-821X(80)90180-6.

Jansma, P., Mattioli, G., Lopez, A., DeMets, C., Dixon, T.H., Mann, P., and Calais, E., 2000, Neotectonics of Puerto Rico and the Virgin Islands, northeastern Caribbean, from GPS geodesy: Tectonics, v. 19, p. 1021–1037, doi: 10.1029/1999TC001170.

Jolly, W.T., and Lidiak, E.G., 2006, Role of crustal melting in petrogenesis of the Cretaceous Water Island Formation (Virgin Islands, northeast Antilles Island Arc): Geologica Acta, v. 4, p. 7–34.

Jolly, W.T., Lidiak, E.G., Schellekens, H.S., and Santos, S., 1998, Volcanism, tectonics, and stratigraphic correlations in Puerto Rico: Geological Society of America Special Paper 322, p. 1–34.

Jolly, W.T., Lidiak, E.G., Dickin, A.P., and Wu, T.-W., 2001, Secular geochemistry of central Puerto Rican island arc lavas: Constraints on Mesozoic tectonism in the Greater Antilles: Journal of Petrology, v. 42, p. 2197–2214, doi: 10.1093/petrology/42.12.2197.

Jolly, W.T., Lidiak, E.G., and Dickin, A.P., 2006, Cretaceous to mid-Eocene pelagic sediment budget in Puerto Rico and the Virgin Islands (northeast Antilles Island Arc): Geologica Acta, v. 4, p. 35–62.

Jolly, W.T., Schellekens, J.H., and Dickin, A.P., 2007, High-Mg andesites and related lavas from southwestern Puerto Rico (Greater Antilles Island Arc): Petrogenetic links with emplacement of the Caribbean mantle plume: Lithos, v. 98, p. 1–26, doi:10.1016./j.lithos.2007.01.011.

Juster, T.C., Grove, T.L., and Perfit, M.R., 1989, Experimental constraints on the generation of Fe-Ti basalts, andesites, and rhyodacites at the Galapagos spreading center: Journal of Geophysical Research, v. 94, p. 9251–9274.

Kaczor, L., and Rogers, J., 1990, The Cretaceous Aguas Buenas and Río Matón limestones of southern Puerto Rico: Journal of South American Earth Sciences, v. 3, p. 1–8, doi: 10.1016/0895-9811(90)90013-Q.

Kepezhinskas, P.K., Defant, M.J., and Drummond, M.J., 1995, Na metasomatism in the island-arc mantle by slab melt-peridotite interaction: Evidence from mantle xenoliths in the North Kamchatka Arc: Journal of Petrology, v. 36, p. 1505–1527.

Kerr, A.C., and Tarney, J., 2005, Tectonic evolution of the Caribbean and northwestern South America: The case for accretion of two Late Cetaceous oceanic plateaus: Geology, v. 33, p. 269–272, doi: 10.1130/G21109.1.

Kerr, A.C., Iturralde-Vinent, M., Saunders, A.D., Babbs, T.L., and Tarney, J., 1999, A new plate tectonic model of the Caribbean: Implications from a geochemical reconnaissance of Cuban Mesozoic volcanic rocks: Geological Society of America Bulletin, v. 111, p. 1581–1599, doi: 10.1130/0016-7606(1999)111<1581:ANPTMO>2.3.CO;2.

Kerr, A.C., Tarney, J., Kempton, P., Spaden, S., Nivia, A., Marriner, G., and Duncan, R., 2002, Pervasive mantle plume head heterogeneity: Evidence from the late Cretaceous Caribbean-Columbian oceanic plateau: Journal of Geophysical Research, v. 107, p. ECV2.

Kerr, A.C., White, R.V., Thompson, M.E., Tarney, J., and Saunders, A.D., 2003, No oceanic plateau—No Caribbean plate? The seminal role of an oceanic plateau in Caribbean plate evolution: American Association of Petroleum Geologists Memoir 79, p. 126–168.

Kesler, S.E., Russell, N., Polanco, J., McCurdy, K., and Cumming, G.J., 1991, Geology and geochemistry of the Los Ranchos formation, central Dominican Republic: Geological Society of America Special Paper 262, p. 187–201.

Kesler, S.E., Campbell, J.H., and Allen, C.M., 2005, Age of the Los Ranchos Formation, Dominican Republic: Timing and tectonic setting of primitive island arc volcanism in the Caribbean region: Geological Society of America Bulletin, v. 117, p. 987–995, doi: 10.1130/B25594.1.

Koepke, J., Feig, S., Snow, J., and Freise, M., 2004, Petrogenesis of oceanic plagiogranites by partial melting of gabbro: An experimental study: Contributions to Mineralogy and Petrology, v. 146, p. 414–432, doi: 10.1007/s00410-003-0511-9.

Koepke, J., Berndt, J., Feig, S.T., and Holtz, F., 2007, The formation of SiO_2-rich melts within the deep oceanic crust by partial melting of gabbros: Contributions to Mineralogy and Petrology, v. 153, p. 67–84.

Lapierre, H., Dupuis, V., Lepinay, B., Bosch, D., Moni, P., Tardy, M., and Maury, R., 1999, Late Jurassic oceanic crust and Upper Cretaceous Caribbean Plateau picritic basalts exposed in the Duarte igneous complex, Hispaniola: Journal of Geology, v. 107, p. 193–207, doi: 10.1086/314341.

Lebron, M., and Perfit, M., 1994, Petrochemistry and tectonic significance of Cretaceous island arc rocks, Cordillera Oriental, Dominican Republic: Tectonophysics, v. 229, p. 69–100, doi: 10.1016/0040-1951(94)90006-X.

Le Maitre, R.W., 1989, A classification of igneous rocks and glossary of terms: Oxford, Blackwell, 193 p.

Lewis, J.F., Hames, W.E., and Draper, G., 1999, Late Jurassic oceanic crust and Upper Cretaceous Caribbean plateau picritic basalts exposed in the Duarte igneous complex, Hispaniola: A discussion: Journal of Geology, v. 107, p. 505–508, doi: 10.1086/314358.

Lidiak, E.G., and Jolly, W.T., 1996, Circum-Caribbean granitoids: Characteristics and origin: International Geology Review, v. 38, p. 1098–1133.

Luchitskaya, M.V., Morozov, O.L., and Palandzhyan, S.A., 2005, Plagiogranite magmatism in the Mesozoic island-arc structure of the Pekulney Ridge, Chykotka Peninsula, NE Russia: Lithos, v. 79, p. 251–269, doi: 10.1016/j.lithos.2004.04.056.

MacPhee, R., Iturralde-Vinent, M.A., and Gaffney, E., 2003, Domo de Zaza, an early Miocene vertebrate locality in south-central Cuba, with notes on the tectonic evolution of Puerto Rico and Mona Passage: American Museum of Natural History Noviates, v. 3394, 42 p.

Malpas, J., 1979, Two contrasting trondhjemite associations from transported ophiolites in Western Newfoundland, *in* Barker, F., ed., Trondhjemites, dacites, and related rocks: Amsterdam, Elsevier, p. 465–487.

Marchesi, C., Garrido, C., Bosch, D., Proenza, J., Gervilla, F., Monié, P., and Rodríguez-Vega, A., 2007, Geochemistry of Cretaceous magmatism in eastern Cuba: Recycling of North American continental sediments and implications for subduction polarity in the

Greater Antilles paleo-arc: Journal of Petrology, v. 48, p. 1813–1840.

Mattson, P.H., 1960, Geology of the Mayagüez area, Puerto Rico: Geological Society of America Bulletin, v. 71, p. 319–362, doi: 10.1130/0016-7606(1960)71[319:GOTMAP]2.0.CO;2.

Mattson, P.H., 1968, Geologic map of the Jayüya quadrangle, Puerto Rico: U.S. Geological Survey Miscellaneous Geological Investigations Map I-520, scale 1:20,000.

Mattson, P.H., 1979, Subduction, buoyant braking, flipping, and strike-slip faulting in the northern Caribbean: Journal of Geology, v. 87, p. 293–304.

McKenzie, D., and O'Nions, R.K., 1991, Partial melt distributions from inversion of rare-earth element concentrations: Journal of Petrology, v. 32, p. 1021–1091.

Miyashiro, A., 1974, Volcanic rock series in island arcs and continental margins: American Journal of Science, v. 274, p. 321–355.

Montgomery, H.A., Pessagno, E., Lewis, J.F., and Schellekens, J.H., 1994, Paleogeography of Jurassic fragments in the Caribbean: Tectonics, v. 13, p. 725–732, doi: 10.1029/94TC00455.

Nichols, G.T., Wylie, P.J., and Stern, C.R., 1994, Subduction zone melting of pelagic sediments constrained by melting experiments: Nature, v. 371, p. 785–788, doi: 10.1038/371785a0.

Pallister, J.S., and Knight, R.J., 1981, Rare-earth element geochemistry of the Samail ophiolite near Ibra, Oman: Journal of Geophysical Research, v. 86, p. 2673–2697.

Pearce, J.A., and Parkinson, I.J., 1993, Trace element models for mantle melting: Application to arc petrogenesis: Geological Society [London], Special Paper 76, p. 373–403.

Pease, M.H., Jr., 1968, Cretaceous and lower Tertiary stratigraphy of the Naranjito and Aguas Buenas quadrangles: U.S. Geological Survey Bulletin 1253, 57 p.

Peccerillo, A., and Taylor, S.R., 1976, Geochemistry of Eocene volcanic rocks from the Kastamonu area, northern Turkey: Contributions to Mineralogy and Petrology, v. 58, p. 63–81, doi: 10.1007/BF00384745.

Pindell, J.L., 2004, Origin of Caribbean plateau basalts and the arc-arc Caribbean-South America collision: The arc-arc Caribbean–South America collision and upper level axis parallel extension in the southern Caribbean plate boundary zone [abstract]: Eos (Transactions, American Geophysical Union), v. 85, no.47, Fall Meeting Supplement, session T33B, abstract 1365.

Pindell, J.L., and Barrett, S.F., 1990, Geological evolution of the Caribbean region: A plate tectonic perspective: Geological Society of America, The Geology of North America, v. H, p. 405–432.

Pindell, J.L., Kennan, L., Stanek, K.P., Maresch, W.V., and Draper, G.G., 2006, Foundations of Gulf of Mexico and Caribbean evolution: Eight controversies resolved: Acta Geologica, v. 4, p. 303–341.

Plank, T., and Langmuir, C.H., 1998, The chemical composition of subducting sediment and its consequences for the crust and mantle: Chemical Geology, v. 145, p. 325–394, doi: 10.1016/S0009-2541(97)00150-2.

Rankin, D.W., 2002, Geology of St. John, U. S. Virgin Islands: U.S. Geological Survey Professional Paper 1631, p. 1–36.

Rapp, R.P., Shimizu, N., Norman, M.D., and Applegate, G.S., 1999, Reaction between slab-derived melts and peridotite in the mantle wedge: Experimental constraints at 3.8 Gpa: Chemical Geology, v. 160, p. 335–356, doi: 10.1016/S0009-2541(99)00106-0.

Révillon, S., Hallot, E., Arndt, N.T., Chauvel, C., and Duncan, R.A., 2000, A complex history for the Caribbean Plateau: Petrology, geochemistry, and geomorphology of the Beata ridge, South Hispaniola: Journal of Geology, v. 108, p. 641–666, doi: 10.1086/317953.

Rollinson, H., 1993, Using Geochemical Data: Evaluation, Presentation, Interpretation: Essex, England, Longman Scientific & Technical, 352 p.

Ryerson, F.J., and Watson, E.B., 1987, Rutile saturation in magmas: Implications for Ti-Nb-Ta depletion in island-arc basalts: Earth and Planetary Science Letters, v. 86, p. 225–239, doi: 10.1016/0012-821X(87)90223-8.

Schellekens, J.H., 1991, Late Jurassic to Eocene geochemical evolution of volcanic rocks of Puerto Rico: Geophysical Research Letters, v. 18, p. 523–556.

Schellekens, J.H., 1998, Geochemical evolution and tectonic history of Puerto Rico: Geological Society of America Special Paper 322, p. 35–66.

Shaw, D.M., 1970, Trace element fractionation during anatexis: Geochimica et Cosmochimica Acta, v. 34, p. 237–243, doi: 10.1016/0016-7037(70)90009-8.

Smith, A.L., Schellekens, J.H., and Díaz, M., 1998, Batholith emplacement in the northeastern Caribbean: Markers of tectonic change: Geological Society of America Special Paper 322, p. 99–122.

Smith, I.E.M., Stewart, R.B., and Price, R.C., 2003, The petrology of a large intra-oceanic silicic eruption: The Sandy Bay tephra, Kermadec Arc, southwest Pacific: Journal of Volcanology and Geothermal Research, v. 124, p. 173–194, doi: 10.1016/S0377-0273(03)00040-4.

Sun, S.-S., and McDonough, W.F., 1989, Chemical and isotopic systematics of oceanic basalts: Geological Society Special Publication 42, p. 313–345.

Tamura, Y., and Tatsumi, Y., 2002, Remelting of andesitic crust as possible origin of rhyolite in oceanic arcs: An example from Izu-Bonin Arc: Journal of Petrology, v. 43, p. 1029–1047, doi: 10.1093/petrology/43.6.1029.

Tatsumi, Y., 2001, Geochemical modeling of partial melting of subducting sediments and subsequent melt-mantle interaction: Generation of high-Mg andesites in the Setouchi volcanic belt, southwest Japan: Geology, v. 29, p. 323–326, doi: 10.1130/0091-7613(2001)029<0323:GMOPMO>2.0.CO;2.

Taylor, B., and Martinez, F., 2003, Back-arc basin systematics: Earth and Planetary Science Letters, v. 30, p. 481–497.

Taylor, S.R., and McLennan, S.M., 1985, The continental crust: Its composition and evolution: Oxford, Blackwell, 314 p.

Thompson, M.E., Kempton, D., White, R.V., Kerr, A.C., Tarney, J., Saunders, A.D., Fritton, J.G., and McBirney, A., 2004, Hf-Nd isotope constraints on the origin of the Cretaceous Caribbean plateau and its relationship to the Galapagos plume: Earth and Planetary Science Letters, v. 217, p. 59–75, doi: 10.1016/S0012-821X(03)00542-9.

Thy, P., and Lofgren, G.E., 1994, Experimental constraints on the low-pressure evolution of transitional and mildly alkalic basalts: The effect of Fe-Ti oxide minerals, and the origin of basaltic andesites: Contributions to Mineralogy and Petrology, v. 116, p. 340–351, doi: 10.1007/BF00306502.

Toplis, M.J., and Carroll, M.R., 1995, An experimental study of the influence of oxygen fugacity on Fe-Ti oxide stability, phase relations, and mineral-melt equilibria in ferro-basalt systems: Journal of Petrology, v. 36, p. 1137–1170.

Tsvetkov, A.A., 1991, Magmatism of the westernmost (Komandorsky) segment of the Aleutian island arc: Tectonophysics, v. 199, p. 289–317, doi: 10.1016/0040-1951(91)90176-S.

van Westrenen W., Blundy, J.D., and Wood, B.J., 2001, High field strength element/rare-earth element fractionation during partial melting in the presence of garnet: Implications for identification of mantle heterogeneities: Geochemistry Geophysics Geosystems, v. 2, no. 2000GC000133.

Yazeva, R.G., 1978, Sodic-acidic volcanites of the Urals and plagiorhyolites of recent island arcs: International Geology Review, v. 20, p. 1009–1020.

Manuscript Received 19 February 2007
Revised Manuscript Received 3 September 2007
Manuscript Accepted 7 September 2007

Printed in the USA